

Electric polarization of one-dimensional inversion-symmetric two-band insulators

Jean-Noël Fuchs^{1,*} and Frédéric Piéchon^{2,†}

¹*Sorbonne Université, CNRS, Laboratoire de Physique Théorique de la Matière Condensée, LPTMC, 75005 Paris, France*

²*Université Paris-Saclay, CNRS, Laboratoire de Physique des Solides, 91405, Orsay, France*

(Dated: May 25, 2022)

The bulk electric polarization P of one-dimensional crystalline insulators is defined modulo a polarization quantum P_q . The latter is a measurable quantity that depends on the number n_s of sites per unit cell. For two-band models, $n_s = 1$ or 2 and $P_q = g/n_s$ ($g = 1$ or 2 being the spin degeneracy). For inversion-symmetric crystals either $P = 0$ or $P_q/2 \bmod P_q$. Depending on the position of the two inversion centers with respect to the ions, three situations arise: bond, site or mixed inversion. As representative two-band examples of these three cases, we study the Su-Schrieffer-Heeger (SSH), charge density wave (CDW) and Shockley models. SSH has a unique phase with $P = 0 \bmod g/2$, CDW has a unique phase with $P = g/4 \bmod g/2$, and Shockley has two distinct phases with $P = 0$ or $g/2 \bmod g$. In all three cases, as long as inversion symmetry is present, chiral symmetry is found to be irrelevant for P . As a generalization of SSH and CDW, we analytically compute P for the RM model and illustrate the role of the unusual $P_q = g/2$ on edge and soliton fractional charges and on adiabatic pumping.

I. INTRODUCTION

The electric polarization P of a one-dimensional (1D) crystalline insulator is a subtle quantity already classically. Because of discrete translation invariance, it is only defined modulo a fixed amount, usually called the “polarization quantum” P_q (even if unrelated to quantum mechanics) [1]. Therefore, the bulk electric polarization of a periodic system is essentially an angle [2]:

$$\vartheta = 2\pi \frac{P}{P_q}. \quad (1)$$

To understand why, consider an ionic chain made of a periodic alternation of cations and anions, that are treated classically as localized point charges (a 1D version of rock salt made of Na^+ and Cl^-). The polarization is the electric dipole moment per unit cell. This quantity depends on the unit cell choice. In order that the polarizations obtained for different choices of unit cell – call them P_1, P_2, \dots – agree, one realizes that they can only be equal in a modulo sense:

$$P_1 = P_2 = \dots \bmod P_q. \quad (2)$$

This defines the polarization quantum P_q . It depends on the Bravais lattice and on the electric charges of the crystal’s constituents.

Now consider a 1D crystal made of cations and mobile electrons and call g the spin degeneracy ($g = 1$ or 2). Usually, ions are treated classically, while electrons are described quantum mechanically. By reasoning on electrons only, the polarization quantum is commonly found to be $P_q = gea/\Omega = g$ [1, 4–8], where $-e = -1$ is the electron charge, Ω is the volume of the unit cell and a is the smallest non-zero Bravais lattice vector, here $\Omega = a$.

However, the polarization quantum is dependent not only on electrons but also on ions, as the polarization only makes sense for an electrically-neutral system. The polarization quantum depends on the number n_s of sites per unit cell. For two-band models, n_s is either 1 or 2 and we find that:

$$P_q = \frac{g}{n_s}. \quad (3)$$

For example, for the Shockley model describing coupled s and p bands [5, 9], in each unit cell there is a single ion of charge g and g electrons. The polarization quantum is then found to be $P_q = g$. However, for the Rice-Mele (RM) model [10] with two ions of charge $g/2$ each and g electrons per unit cell, the polarization quantum turns out to be $P_q = g/2$. We give a proof of that key result and emphasize that the polarization quantum is not a matter of choice or nomenclature, but is a physical quantity and we propose a way to measure it from end charges in long open chains.

In the absence of a protecting symmetry, there is a single class of 1D band insulators [11–13]. However, for a crystal with inversion symmetry, the bulk polarization P must satisfy $P = -P \bmod P_q$ and therefore either $P = 0$ or $P_q/2 \bmod P_q$ [5, 14–16]. This allows one to distinguish two classes of inversion-symmetric insulators depending on whether

$$\vartheta = 0 \text{ (trivial) or } \pi \text{ (topological)}, \quad (4)$$

the angle ϑ acting as a \mathbb{Z}_2 invariant. Actually, any symmetry (not just inversion) that makes $P = -P \bmod P_q$ leads to these two classes. See [17], for an example involving particle-hole symmetry.

In this article, we study three different flavors of inversion-symmetric insulators, depending on the position of the two inversion centers per unit cell with respect to the ions. The inversion centers can be both on-site (site inversion) or both mid-bond (bond inversion) or one on-site and the other mid-bond (mixed inversion).

* fuchs@lptmc.jussieu.fr

† piechon@lps.u-psud.fr

As examples of the three cases, we use two-band models: the charge density wave (CDW, site inversion) chain, the Su-Schrieffer-Heeger (SSH, bond inversion) chain [18] and the Shockley model (mixed inversion). The first two are special cases of the RM model in which either the dimerization or the staggered on-site potential vanishes.

The gap-closing phase transitions that occur as a function of a control parameter in these three models are of different nature. Indeed, in the three cases and at the transition, the inversion symmetry is of mixed type. In

other words, only for the Shockley model does the inversion symmetry remain of the same flavor across the transition, whereas for CDW and SSH it is different flavor at the transition. We find that CDW has a unique gapped phase with quantized polarization, that SSH has a unique gapped phase with vanishing polarization and that Shockley has two distinct gapped phases, one trivial with vanishing polarization and the other topological with quantized polarization. Our findings are summarized in Table I.

	SSH	SSH	CDW	CDW	Shockley	Shockley
phase	$\delta > 0$	$\delta < 0$	$\Delta > 0$	$\Delta < 0$	$\epsilon_p - \epsilon_s > 2(t_{pp} - t_{ss})$	$\epsilon_p - \epsilon_s < 2(t_{pp} - t_{ss})$
inversion centers	mid-bonds	mid-bonds	on-sites	on-sites	mixed	mixed
ions' position	2c	2c	1a and 1b	1a and 1b	1a	1a
Wannier center (electrons' position)	mid-bond	mid-bond	on-site	on-site	on-site	mid-bond
P_q	$g/2$	$g/2$	$g/2$	$g/2$	g	g
P modulo P_q	0	0	$P_q/2 = g/4$	$P_q/2 = g/4$	0	$P_q/2 = g/2$
$\vartheta = 2\pi P/P_q$	0	0	π	π	0	π
insulator type	molecular	molecular	ionic	ionic	atomic	covalent

TABLE I. Three types of inversion-symmetric insulators illustrated by the SSH, CDW and Shockley models. The notations 1a, 1b and 2c refer to particular positions in the unit cell, known as Wyckoff positions, see Fig. 1. The two inversion centers are always at 1a and 1b, but they can be both on-site, or both mid-bond, or mixed (one on-site and one mid-bond). At the transition, inversion symmetry is of mixed type in all three cases.

That SSH has a unique gapped phase with vanishing polarization agrees with [16, 19] but disagrees with the commonly held view that SSH has two distinct gapped phases, one that is trivial and the other that is topological, see e.g. [13, 15, 22–28].

The article is organized as follows: in Sec. II, we first define the RM model, and discuss in particular its two inversion-symmetric limits that are the CDW and SSH chains. Next, in Sec. III, we prove that the polarization quantum of RM is twice smaller than usually assumed, analytically compute the bulk electric polarization and check this result by numerically studying the polarization of open chains. In Sec. IV, we study the charge accumulation at edges or interfaces and its relation to the bulk polarization and discuss the gap-closing transitions that occur in SSH and CDW. In Sec. V, we compare CDW and SSH to the Shockley model of coupled s and p bands and show that the latter has a simpler behavior as an inversion-symmetric insulator. Eventually, the consequences of the unusual polarization quantum on adiabatic pumping in RM are presented in Sec. VI. We then conclude in Sec. VII. In Appendices, we give calculation details for the polarization (Sec. A) and discuss the chiral symmetry of the SSH model (Sec. B).

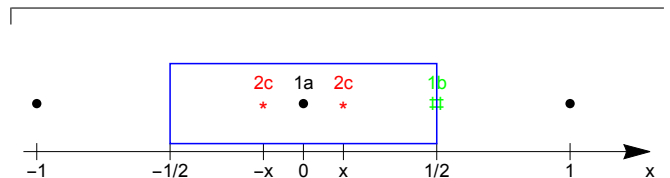


FIG. 1. Wyckoff positions of the one-dimensional inversion-symmetric lattice: 1a, 1b and 2c. If the chosen inversion center is at $x = 0$, then 1a is $x = 0 \bmod 1$, 1b is $x = 1/2 \bmod 1$ and 2c is any $x \neq 0$ and $\neq 1/2 \bmod 1$ such that under inversion $x \rightarrow -x \neq x \bmod 1$. The unit cell is shown as a blue rectangle.

II. RICE-MELE MODEL

A. Tight-binding model

The RM model is a one-dimensional tight-binding model with two sites A and B per unit cell at position x_A and x_B . The lattice spacing a is taken as unit length. Each site $j = (R, l)$ contains a single s orbital $|j\rangle$, where $l = A, B$ labels the sublattices and R is an integer that spans the Bravais lattice. The tight-binding Hamiltonian

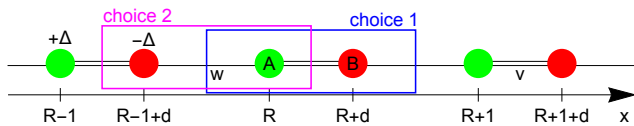


FIG. 2. The RM model for a generic distance d between A and B sites. The two hopping amplitudes are $v = 1 + \delta$ and $w = 1 - \delta$, where δ is the dimerization. The on-site energies are $\pm\Delta$. Two possible choices of unit cell are indicated.

is called H . Its two nearest-neighbor hopping amplitudes are $v = t(1 + \delta)$ (strong bond if the dimerization $\delta > 0$) and $w = t(1 - \delta)$ (weak bond if $\delta > 0$) and the staggered on-site potential is Δ , following the pattern shown in Fig. 2. Without loss of generality, we assume that v and w are ≥ 0 and take energy units such that $t = 1$. The position operator reads

$$x = \sum_j x_j |j\rangle\langle j|, \quad (5)$$

with $x_j = x_A = R$ if $j = (R, A)$ and $x_j = x_B = R + d$ if $j = (R, B)$ and the A - B distance is called d (see Fig. 2). Physically, the strongest bond should have a shorter distance and d should be a function of the dimerization strength δ , such that $d = 1/2$ when $\delta = 0$ and $d < 1/2$ when $\delta > 0$. For example, using Harrison's law

$$\begin{aligned} H_d(k) &= [v \cos(kd) + w \cos(kd - k)] \sigma_x + [v \sin(kd) + w \sin(kd - k)] \sigma_y + \Delta \sigma_z \\ &= 2 \cos \frac{k}{2} \sigma_x^{\text{eff}}(k, d) + 2\delta \sin \frac{k}{2} \sigma_y^{\text{eff}}(k, d) + \Delta \sigma_z, \end{aligned} \quad (6)$$

with the effective Pauli matrices

$$\sigma_j^{\text{eff}}(k, d) = e^{i\phi\sigma_z/2} \sigma_j e^{-i\phi\sigma_z/2}, \quad (7)$$

where $\phi = k(d - 1/2)$ and $j = x, y, z = 1, 2, 3$. When $d = 1/2$, we simply call $H(k) = H_{1/2}(k)$ the Bloch Hamiltonian and $\sigma_j^{\text{eff}} = \sigma_j$ are the standard Pauli matrices. The eigenvectors of (6) are cell-periodic Bloch states $|u_n(k)\rangle$ with band index $n = \pm$ and wavevector k in the first Brillouin zone $[-\pi, \pi[$. The corresponding eigenvalues are

$$E_{\pm}(k) = \pm \sqrt{4 \cos^2 \frac{k}{2} + 4\delta^2 \sin^2 \frac{k}{2} + \Delta^2}, \quad (8)$$

and do not depend on d .

We assume that the model is half-filled, so that when it is gapped, it describes a band insulator. For spinless electrons (spin degeneracy $g = 1$), it means that there is a single electron per unit cell. For spinful electrons ($g = 2$), there are two electrons per unit cell. The number of electrons is therefore $gN/2$ if there are N (even) sites corresponding to $N/2$ unit cells. For a finite system, k takes $N/2$ discrete values $n2\pi/L$, where n is an integer.

for the relation between hopping amplitude and distance, one could take $d = (2 + \delta)/4$. However, the model with $d = 1/2$ for all δ already contains the essential features and we shall often consider this special case.

The system has translation invariance: it is either infinite or finite with periodic boundary conditions (PBC). In this last case, it contains N sites, has a length $L = N/2$ and we need to be careful in treating the position operator. Indeed, the above operator (5) is not correct, as it does not capture the fact that $x_j + L \equiv x_j$, see the nice discussion by Resta [20].

Following [5], we introduce the angle θ such that $\Delta = M \cos \theta$ and $\delta = M \sin \theta$ with $M \equiv \sqrt{\Delta^2 + \delta^2} > 0$. This angle is a convenient parametrization of the RM model. In practice, we will essentially change θ and not so much M . This angle θ should not be mistaken for $\vartheta = 2\pi P/P_q$.

B. Bloch Hamiltonian

The (canonical) Bloch Hamiltonian is obtained from the unitary transformation $e^{-ikx} H e^{ikx}$ of the tight-binding Hamiltonian H , where x is the position operator and k a number. Because of translation invariance and of the Bloch theorem, after projection on a sub-space at fixed k , it becomes a 2×2 matrix that reads

C. Symmetries

In this section, we discuss several symmetries of RM:

Time-reversal symmetry.— The RM model has time-reversal symmetry $H_d(-k)^* = H_d(k)$, which implies that $E_n(-k) = E_n(k)$.

Pseudo-charge conjugation.— The Bloch Hamiltonian also obeys the following relation

$$\sigma_y H_d(-k) \sigma_y = -H_d(k), \quad (9)$$

which implies that $E_-(k) = -E_+(-k)$. This is a peculiar transformation as it anticommutes with the Hamiltonian. However, it is neither a chiral symmetry (as it involves k) nor a charge conjugation (as it is not anti-unitary, it does not involve complex conjugation). In real space, it is a kind of inversion with respect to a mid-bond center. If we take the latter as position origin, it acts as

$$\begin{aligned} |R, A\rangle &\rightarrow |i| - R, B\rangle \\ |R, B\rangle &\rightarrow |-i| - R, A\rangle, \end{aligned} \quad (10)$$

on the real-space orbitals $|R, l\rangle$. Together with time-reversal symmetry, Eq. (9) implies that $E_-(k) = -E_+(k)$, i.e. it explains the $E \rightarrow -E$ symmetry of the energy spectrum, see Eq. (8). This is actually true of any two-band model that involves only the three Pauli matrices and not the identity σ_0 .

Inversion symmetry.— Generally speaking, the RM model does not have inversion symmetry. However, there are three particular values of the parameters for which inversion symmetry is present but in different guise.

(i) *Bond inversion:* First, the SSH model corresponds to $\Delta = 0$ and $\delta \neq 0$ (i.e. $\theta = \pi/2$ or $3\pi/2$). It is a two-band insulator with a gap due to the dimerization. The two inversion centers per unit cell are mid-bond ($\bar{x} = (x_A + x_B)/2$ and $\bar{x} + 1/2$). Inversion symmetry acts as

$$H_d(k) \rightarrow \sigma_x H_d(-k) \sigma_x = H_d(k) \text{ when } \Delta = 0. \quad (11)$$

(ii) *Site inversion:* Second, the charge density wave (CDW) or binary chain corresponds to $\delta = 0$ and $\Delta \neq 0$ (i.e. $\theta = 0$ or π). In that case, necessarily $d = 1/2$. It is also a two-band insulator with a gap due to the staggered on-site potential. The two inversion centers per unit cell are on-site (x_A and x_B). In that case, inversion symmetry acts as

$$H(k) \rightarrow H(-k) = H(k) \text{ when } \delta = 0. \quad (12)$$

(iii) *Mixed inversion:* Third, if $\delta = 0$ and $\Delta = 0$, this is a single-band gapless system and the two inversion centers are mid-bond and on-site. It describes a 1D metal in the absence of Peierls instability. For future reference, we note that the Shockley model, discussed in Sec. V, also has inversion centers of mixed type. This will play an important role in the comparison between the three different types of inversion-symmetric insulators: SSH, CDW and Shockley.

Chiral symmetry.— The RM model does not, in general, have chiral symmetry. However, when $\Delta = 0$, the SSH model is bipartite and there is a chiral (sublattice) symmetry, which means that:

$$\sigma_z H_d(k) \sigma_z = -H_d(k). \quad (13)$$

When $\delta = 0$, the CDW model has another chiral symmetry:

$$\sigma_y H(k) \sigma_y = -H(k). \quad (14)$$

In summary, SSH is a chiral and bond inversion-symmetric insulator, CDW is a chiral and site inversion-symmetric insulator and Shockley is a mixed inversion-symmetric insulator. For generic parameters, RM is a band insulator without inversion or chiral symmetry.

D. Relabelling symmetry: single bulk SSH phase

The SSH model has a *single* gapped phase and not two as often assumed. For an SSH chain on a circle (i.e. with

PBC), it is obvious that taking one dimerization or the other makes no difference. In the bulk (i.e. either an infinite chain or a finite chain with PBC), the two dimerizations ($\delta > 0$ and $\delta < 0$) are equivalent by a translation by half a Bravais lattice vector. As a consequence, any bulk physical quantity must be the same for $\delta > 0$ and $\delta < 0$. The two dimerizations are only distinguished for a chain with an edge or by a domain wall (similar to a grain boundary in a crystal). The two dimerizations actually result from the spontaneous symmetry breaking of a \mathbb{Z}_2 symmetry. In analogy, an Ising ferromagnet pointing in two opposite directions is not considered as two different phases of matter.

Likewise, the CDW chain has a single gapped phase in the bulk and it does not matter whether $\Delta > 0$ or $\Delta < 0$. More generally, the RM model is invariant under the following parameter transformation $(d, \Delta, \delta) \rightarrow (1 - d, -\Delta, -\delta)$ and relabeling of the two sublattices ($A \leftrightarrow B$). On the Bloch Hamiltonian $H_{d,\Delta,\delta}(k)$ in Eq. (6), this symmetry acts as:

$$H_{d,\Delta,\delta}(k) \rightarrow \sigma_x H_{1-d,-\Delta,-\delta}(k) \sigma_x = H_{d,\Delta,\delta}(k). \quad (15)$$

Without loss of generality, one may therefore restrict the study of the RM model to $\delta \geq 0$ (and correspondingly to $0 \leq d \leq 1/2$), i.e. to $0 \leq \theta < \pi$ instead of $0 \leq \theta < 2\pi$.

III. ELECTRIC POLARIZATION

The electric polarization is the dipole moment per unit length of a neutral insulating system. By default, we shall be concerned with the bulk polarization, i.e. the polarization for a periodic system (either infinite or finite with PBC) without edges. The bulk polarization will be denoted P . When we will consider a finite and open system with edges, we will use P_{open} to denote the polarization.

If we consider spinless electrons ($g = 1$), there should be a single electron of charge $-e = -1$ per unit cell for the RM model to be half-filled, i.e. to be a bulk band insulator (in the following charges are all measured in units of e). For the system to be neutral, the two ions in the unit cell should therefore carry a total charge of $+1$. In order to have inversion symmetry in the SSH limit, in which $A \leftrightarrow B$, the two ions should be equally charged and therefore each carry a charge of $+1/2$. This fixes the electric charge of ions in the spinless case. If we consider spinful electrons ($g = 2$), there should be two electrons per unit cell and the ions should carry a $+1$ charge each. In the end, each ion carries a charge $+g/2$. The spinful case is precisely the model studied by Vanderbilt and King-Smith [5], see also [7, 21]. In the following, we prove that the polarization quantum was not correctly identified in these works.

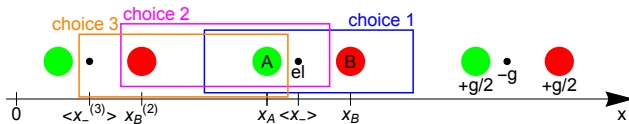


FIG. 3. Polarization quantum for the RM model obtained from three possible choices of unit cell. Each ion carries a charge $+g/2$ and there are g electron per unit cell (with total charge $-g$), which are here represented by the Wannier center $\langle x_- \rangle$, where $g = 1$ or 2 is the spin degeneracy. The lattice spacing is $a = 1$ and the $A - B$ distance is $d = x_B - x_A$.

A. Polarization quantum: twice smaller

An essential feature of the modern theory of polarization is that the bulk polarization P of a crystal is only defined modulo a polarization quantum P_q [1, 4, 6]. Bulk polarization of a crystal refers to a situation in which there is translation invariance, either in a finite or an infinite chain with PBC. Below, we argue that the polarization quantum of the RM model is $P_q = g/2$ and not g .

Indeed, consider the polarization computed in [5, 21] for the RM model parametrized by θ at fixed M (see in particular Fig. 4 in [5] and Fig. 3 in [21]). In the four cases that have inversion symmetry ($\theta = 0, \pi/2, \pi, 3\pi/2$), the polarization is found to be $-g/4, 0, g/4$ and $g/2$. But a centro-symmetric crystal must satisfy $P = -P \bmod P_q$, which means that $P = m \times P_q/2$, where $m \in \mathbb{Z}$. We therefore have to conclude that $P_q = g/2$ such that $0 \equiv g/2$ and $g/4 \equiv -g/4$. Below, we prove that this is indeed the correct value.

In order to find the polarization quantum, we consider several choices of unit cell in the RM model and compare the obtained bulk electric polarizations. Ions are treated as localized (static) classical particles of charge $+g/2$ at position x_j . For electrons, we use the “localization prescription” [1, 5, 6] that the electron charge should be localized at the Wannier (or band) center $\langle x_- \rangle$ of the occupied band (with band index $n = -$). The Wannier center is

$$\langle x_n \rangle = \langle w_{n,0} | x | w_{n,0} \rangle = \int dx x |w_{n,0}(x)|^2, \quad (16)$$

where $w_{n,0}(x) = \langle x | w_{n,0} \rangle$ is the Wannier function

$$w_{n,R}(x) = \int_{\text{BZ}} \frac{dk}{2\pi} e^{-ikR} \psi_{nk}(x)$$

for the n^{th} band in the unit cell such that $R = 0$ (see e.g. [8]). The Wannier center is a position and therefore depends on the position origin. It is defined modulo a lattice spacing $a = 1$.

The Wannier center is also related to the Zak phase Z_n by $\langle x_n \rangle = Z_n/(2\pi)$ [14]. The latter is a special kind of Berry phase – an open-path Berry phase – defined for

a given band by

$$Z_n = \int_{-\pi}^{\pi} dk \langle u_n | i \partial_k u_n \rangle, \quad (17)$$

along a non-contractible loop of the Brillouin zone, where the cell-periodic Bloch states $|u_n(k)\rangle$ are eigenvectors of the canonical Bloch Hamiltonian $H(k)$ and must satisfy the periodic gauge choice $|u_n(k+G)\rangle = e^{-iGx} |u_n(k)\rangle$, where x is the position operator and G a reciprocal lattice vector [29]. Through the periodic gauge choice, the Zak phase depends on the position origin and is defined modulo 2π . This is not surprising as the Wannier center is a position and as such varies continuously with the position origin. The above expression for the Zak phase is valid for a chain with PBC and in the thermodynamic limit in which $\Delta k = 2\pi/L \rightarrow 0$, where the length of the chain $L = N/2$. Generally speaking, the Zak phase is not π times a winding number.

The localization prescription means that the original quantum mechanical problem involving electronic wavefunctions is mapped onto a system of effective point charges, that can be studied by classical electrostatics. The electric polarization is then given as the sum of the electronic and ionic contributions $P = P_{\text{electrons}} + P_{\text{ions}}$. In a given unit cell choice (called choice 1 in Fig. 3), the polarization reads

$$P_1 = -g \langle x_- \rangle + \frac{g}{2} (x_A + x_B) = -g \frac{Z_-}{2\pi} + g \bar{x}, \quad (18)$$

where $\bar{x} = (x_A + x_B)/2$ is the mean ion position in the unit cell. In another unit cell choice (choice 2 in Fig. 3) with the same A ion, and the same Wannier center for the electrons, but another B ion with position $x_B^{(2)} = x_B - 1$, it reads:

$$P_2 = -g \langle x_- \rangle + \frac{g}{2} [x_A + x_B^{(2)}] = P_1 - \frac{g}{2}. \quad (19)$$

If, as a third choice (choice 3 in Fig. 3), we further move the unit cell to the left in order to change the Wannier center such as $\langle x_-^{(3)} \rangle = \langle x_- \rangle - 1$, then:

$$P_3 = -g \langle x_-^{(3)} \rangle + \frac{g}{2} [x_A + x_B^{(2)}] = P_2 + g. \quad (20)$$

We leave it to the reader to check that other unit cell choices always lead to polarizations that differ by an integer multiple of $g/2$, which shows that the polarization quantum is indeed $P_q = g/2$. This value agrees with [19], who studied polyacetylene (corresponding to the spinful SSH chain) and a binary chain equivalent to the spinful CDW model. In the end, the correct formula for the bulk polarization is:

$$P = -g \langle x_- \rangle + g \bar{x} = -g \frac{Z_-}{2\pi} + g \bar{x} \bmod \frac{g}{2}. \quad (21)$$

Why was the polarization quantum wrongly assumed to be g by several authors [5, 7, 21] (including us)? A plausible reason is as follows. For clarity, consider spinless electrons ($g = 1$) and imagine choosing the position

origin such that the ionic contribution to the polarization vanishes, i.e. $\bar{x} = 0$ (this is not the choice made in Fig. 2, where $\bar{x} = d/2$ modulo 1 in the unit cell choice 1). In other words, the position origin is chosen exactly at mid-distance between the two ions in the unit cell. Then the total electric polarization reads

$$P_{\bar{x}=0} = -\langle x_- \rangle = -\frac{Z_-}{2\pi}, \quad (22)$$

and seems to depend only on the electronic contribution. As Wannier centers are defined modulo a lattice spacing $a = 1$, it appears that the polarization is defined modulo 1. But in this process, we have forgotten that it is actually possible to move a charge smaller than an electron (namely a single ion of charge $+1/2$) by one lattice spacing when displacing the unit cell. Here it appears crucial that there are two ions and not a single ion per unit cell, as in the case of the Shockley model that we discuss in Sec. V. In particular, the polarization quantum is here set by the ion charge and not by the electron charge. It is therefore not correct to assume, in general, that the polarization quantum is simply given by the modulo 2π in the Zak phase or equivalently by the modulo $a = 1$ in the Wannier center.

From now on, in the RM model (including SSH and CDW), P_q will mean $g/2$.

B. Bulk polarization: π -periodic in θ

The bulk polarization was computed numerically in Refs. [5, 7, 21] assuming that the polarization quantum was g . It should be modified in order to account for the proper polarization quantum $P_q = g/2$. Here, we first compute it numerically for a finite chain of length $L = N/2$ with an even number of sites N using PBC and restrict to the case $d = 1/2$. Later, we will compute it analytically in the thermodynamic limit. Calling $|\psi_{n,k}\rangle$ the Bloch eigenstates of the tight-binding Hamiltonian H , the electric polarization (21) reads

$$P = -\frac{g}{2\pi} \text{Im} \ln \prod_{k=-\pi}^{\pi-\Delta k} \langle \psi_{-,k+\Delta k} | e^{i\Delta k x} | \psi_{-,k} \rangle + g\bar{x} \quad (23)$$

modulo P_q , where $\Delta k = 2\pi/L$, x is the position operator (5) and $|\psi_{n,\pi}\rangle = |\psi_{n,-\pi}\rangle$. In Eq. (23), the electronic contribution to the polarization is a discretized version [20] of the Zak phase (17). The resulting polarization is shown as a blue curve in Fig. 4(a). The result does not depend much on the system size N and the thermodynamic limit is easily reached. The polarization at $N = 100$ differs from that in the thermodynamic limit (see below) by at most $6 \cdot 10^{-5} P_q$.

Equation (23) can also be computed analytically in the

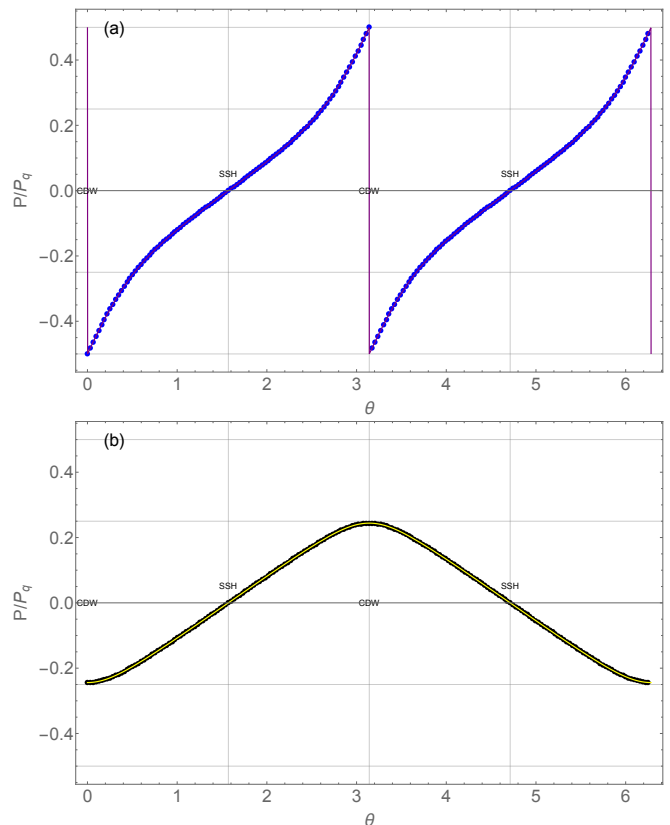


FIG. 4. Bulk electric polarization (in units of the polarization quantum $P_q = g/2$) as a function of θ for the RM model with $M = 0.6$. (a) Blue dots are P obtained from the discretized Zak phase (23) computed on a finite chain of 100 sites with periodic boundary conditions. The purple line is the exact bulk result from the Zak phase in the thermodynamic limit, Eq. (24). (b) Black dots are P_{cell} obtained from the charge density for the same chain. The yellow line is the thermodynamic limit, Eq. (30).

thermodynamic limit $N \rightarrow \infty$ giving

$$P = -\frac{g}{4} [1 - \text{sgn } \delta] \quad (24)$$

$$+ \frac{\Delta\delta}{\pi\sqrt{1 + \Delta^2/4}} \Pi \left(1 - \delta^2, \frac{1 - \delta^2}{1 + \Delta^2/4} \right) \Big] \text{ mod } P_q,$$

where $\Pi(n, m)$ is the complete elliptic integral of the third kind (see Appendix A for details). It is plotted as a purple line in Fig. 4(a). When $|\Delta|$ and $|\delta| \ll 1$, it simplifies to

$$P \approx -\frac{g}{4} \left[1 - \text{sgn } \delta + \frac{2}{\pi} \arctan \frac{\Delta}{2\delta} \right] \text{ mod } P_q, \quad (25)$$

an expression which we will encounter again when discussing soliton charges in Sec IV.

We note that

$$P(\Delta, \delta) + P(\Delta, -\delta) = 0 \text{ mod } P_q, \quad (26)$$

as a consequence of a 2D version of inversion symmetry [see the discussion below Eq. (52)]. We also see that

$$P(-\Delta, -\delta) = P(\Delta, \delta) \text{ mod } P_q, \quad (27)$$

in agreement with the relabelling symmetry. After taking the proper modulo, the polarization is π -periodic as a function of θ , as it should in order to respect the relabelling symmetry. In particular, we see that $P(\theta = 0) = P(\theta = \pi) = P_q/2 [P_q]$ is the value for the CDW chain and $P(\theta = \pi/2) = P(\theta = 3\pi/2) = 0 [P_q]$ is the value for the SSH chain. In other words, CDW has a quantized polarization and SSH a vanishing polarization.

For a chain with PBC, the electric polarization should not be computed from the standard classical formula

$$P_{\text{cell}} = \frac{1}{\Omega} \int_{\text{unit cell}} dx x \rho(x) = \sum_{j=A,B} x_j q_j, \quad (28)$$

which we call the cell polarization. It involves only the charge density $\rho(x) = \sum_j \delta(x - x_j) q_j$, with the charge q_j at site j being the sum of electronic and ionic contributions:

$$q_j = q_j^{\text{el}} + q_j^{\text{ions}} = -g \sum_{k=-\pi}^{\pi-\Delta k} |\psi_{-,k}(x_j)|^2 + \frac{g}{2}. \quad (29)$$

The problem with the above formula is that the naive position operator x is not properly defined on a chain with PBC [20]. Such a naive electric polarization is only correct in the absence of translation-invariance (i.e. for molecules, even very long ones) but can not be applied to the periodic case. This fact is actually at the origin of the crisis that ended with the construction of the modern theory of polarization [5, 6]. The latter showed that the electronic contribution to the polarization must be computed from the Zak phase (i.e. from the phase of the Bloch wavefunctions) and not from the density (i.e. the modulus square of the wavefunctions) [31]. The black dots in Fig. 4(b) represent this naive electric polarization in the case of a chain with PBC and $N = 100$ sites. The yellow line in Fig. 4(b) is the result in the thermodynamic limit, which reads

$$\begin{aligned} P_{\text{cell}} &= (x_B - x_A) q_B^0 \\ &= -\frac{g}{4} \frac{\Delta}{\pi \sqrt{1 + \Delta^2/4}} K \left(\frac{1 - \delta^2}{1 + \Delta^2/4} \right), \end{aligned} \quad (30)$$

where $K(m) = \Pi(0, m)$ is the complete elliptic integral of the first kind, q_B^0 is the charge on a B site and $x_B - x_A = d = 1/2$ (see Appendix A for calculation details). It is very different from the correct result, Eq. (24). In particular, it is not π -periodic and therefore does not respect the relabelling symmetry that it should. In the next section, we study open chains, for which formula (28) may be employed. The study of finite open chains will make it clear that the above formula (30) is not correct for a periodic chain.

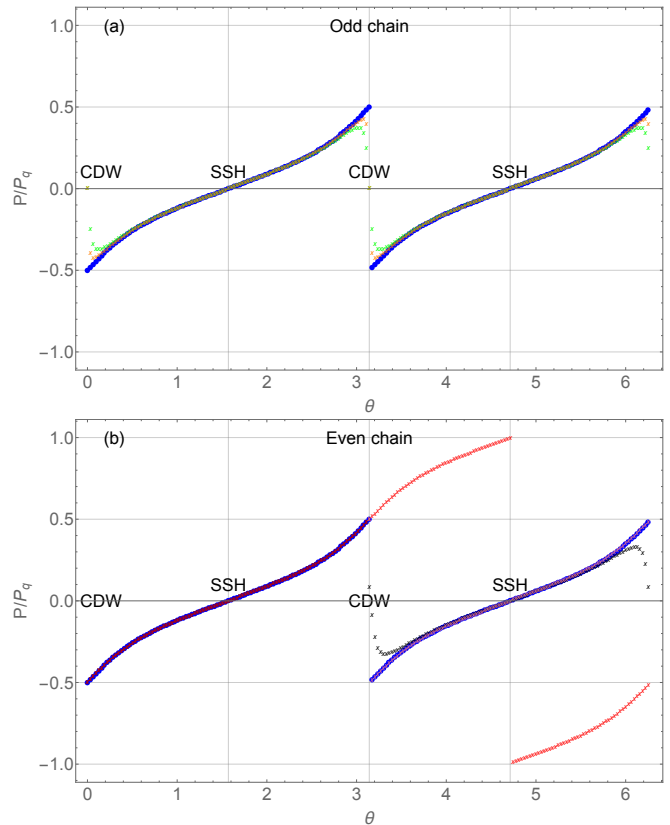


FIG. 5. Electric polarization (in units of the polarization quantum $P_q = g/2$) as a function of θ for a finite chain of the spinful RM model with $M = 0.6$. Blue dots are P for 100 sites with periodic boundary conditions. (a) Green (orange) symbols are P_{open} for 101 (301) sites with open boundary conditions. Compare with Fig. 4 in [5]. (b) Red symbols are P_{open} for 100 sites with open boundary conditions (in pink same data taken modulo P_q ; in black alternative filling when $\pi < \theta < 2\pi$, see text). Compare with Fig. 3 in [21].

C. Polarization for open chains: π or 2π -periodic in θ

In order to better understand the bulk electric polarization, the thermodynamic limit and the appearance of a polarization quantum for a translation-invariant chain (PBC), we study the electric polarization of chains with open boundary conditions (OBC). We need to consider separately chains with an even or an odd number of sites N . Their length is $L = (N - 1)/2$. Chains with an even number of sites have an integer number of units cells, do not have the same number of weak and strong bonds, and can be studied either for the spinless or spinful case, as they always have an integer number of electrons $gN/2$. Chains with an odd number of sites do not have an integer number of unit cells, have as many strong bonds as weak bonds and must be studied for the spinful case in order to have an integer number of electrons $gN/2 = N$. The spinless case can not be studied as there is a conflict

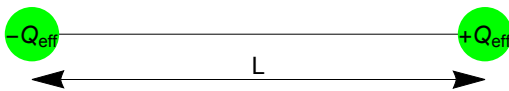


FIG. 6. A one-dimensional insulating and charge-neutral open chain with polarization P_{open} can be modeled as a neutral rod of length L with surface charges $+Q_{\text{eff}}$ and $-Q_{\text{eff}}$ at the two ends. Its dipole moment is $\mu = Q_{\text{eff}}L$ and the effective charge is chosen such as to give the same polarization $\frac{\mu}{L}$, i.e. $Q_{\text{eff}} = P_{\text{open}}$. See Ref. [19].

between charge neutrality and the number of electrons being an integer. For simplicity, in the following, we only consider the spinful case ($g = 2$), so that we can study both the even and odd N cases, and take $d = 1/2$.

For a chain with OBC, we can compute the electric polarization from the electronic charge density, without involving the Zak phase. Calling $|\psi_\alpha\rangle$ the eigenstates of the tight-binding Hamiltonian (with $\alpha = 1, \dots, N$), the polarization reads

$$P_{\text{open}} = \frac{1}{L} \int dx x \rho(x) \quad (31)$$

$$= \frac{1}{L} \left(-g \sum_{\alpha \text{ occ.}} \sum_{j=1}^N x_j |\psi_\alpha(x_j)|^2 + \frac{g}{2} \sum_{j=1}^N x_j \right),$$

where x_j are the positions of ions and $\rho(x) = \sum_{j=1}^N \delta(x - x_j) q_j$ is the charge density. In the electronic term, we need to sum only over occupied states (see below). There is no polarization quantum for a finite chain; the polarization is absolute ($P_{\text{open}} \in \mathbb{R}$) and not defined with a modulo ($P \in] -P_q/2, P_q/2[$).

Actually, this polarization P_{open} can also be interpreted as the end or surface charge of the open chain when it is very long. Indeed, in the thermodynamic limit, the open chain is equivalent to a neutral rod of length L with point charges $\pm Q_{\text{eff}}$ at the two ends, the end charge being chosen such as to give the exact same polarization: $P_{\text{open}} = \mu/L$, with dipole moment $\mu = Q_{\text{eff}}L$ and therefore $P_{\text{open}} = Q_{\text{eff}}$ [19], see Fig. 6. In Sec. IV, we will discuss the end charge Q computed directly from the charge density. We give different names Q and Q_{eff} to these two definitions of the end charge in order to distinguish them, although it will turn out that they become equal in the thermodynamic limit.

In the following, we first discuss the N odd case and then the even case.

1. Odd chain

When N is odd, the energy spectrum does not have $E \rightarrow -E$ symmetry. The $(N-1)/2$ states with lowest energy are all doubly occupied (because of spin degeneracy) and there is one in-gap edge state at energy $\Delta = M \cos \theta$, that contains a single electron, i.e. it is

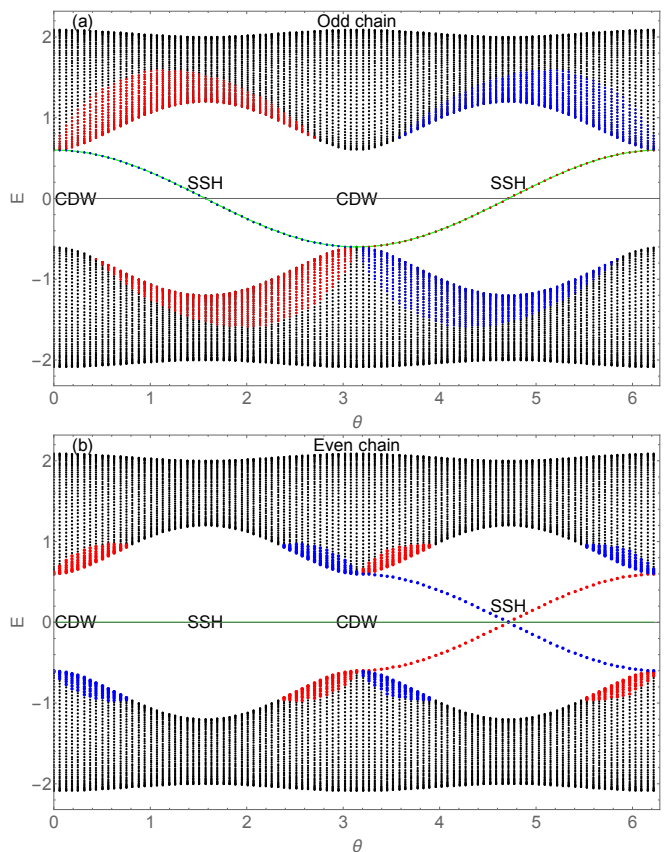


FIG. 7. Energy spectrum for open chains of the RM model with $M = 0.6$ as a function of θ . The length $L = (N-1)/2$ and the number of sites (a) $N = 101$ or (b) $N = 100$. Bulk states ψ_α have a participation ratio above 33% that does not scale with N and are very similar to that obtained for a periodic chain (PBC). Their eigenenergies are shown in black, red or blue if their mean position is in the middle ($0.99L/2 < \langle x_j \rangle_\alpha < 1.01L/2$), on the left ($\langle x_j \rangle_\alpha < 0.99L/2$) or on the right ($\langle x_j \rangle_\alpha > 1.01L/2$) of the chain. In-gap edge states have a participation ratio below 33% and that scales as $1/N$. Their eigenenergies are shown in red when they are located on the left edge ($\langle x_j \rangle_\alpha < L/4$) and in blue when on the right edge ($\langle x_j \rangle_\alpha > 3L/4$). For the even chain, the Fermi level (shown in green) is at zero energy, whereas for the odd chain, it follows the edge state, which is half-filled.

half-filled [see Fig. 7(a)]. The energy of this in-gap state evolves with θ and changes sign. The sum over α in (32) should be understood as $N = (\sum_{\alpha=1}^{(N-1)/2} g) + 1$, where the $+1$ corresponds to the state $\alpha = (N+1)/2$, which is half-filled.

The resulting polarization is plotted in Fig. 5 (a). We see that the polarization looks very much like the PBC result. In particular, it also has the π -periodicity with θ and because it remains between $-g/4$ and $g/4$, it suggests the existence of a polarization quantum in the thermodynamic limit. Finite size effects are visible when θ is close to 0 or π . In the thermodynamic limit, the polarization obtained from the open odd chain tends to the bulk po-

larization [compare the 301 chain with the 101 chain in Fig. 5(a)].

The polarization vanishes exactly at the CDW point in apparent contradiction with the bulk result $P = P_q/2 [P_q]$. The discrepancy is due to the fact that the odd chain has a perfect inversion symmetry when $\theta = 0$ or π . Inversion symmetry for an open chain implies that $P_{\text{open}} = -P_{\text{open}}$ without modulo, so that $P_{\text{open}} = 0$. The abrupt jump that builds in the thermodynamic limit near the CDW point is due to the single electron in the edge state changing from one edge to the other, i.e. a charge -1 that moves by a distance L resulting in a polarization change of $\Delta P_{\text{open}} = (1 \times L)/L = 1 = P_q$.

2. Even chain

When N is even, the energy spectrum has $E \rightarrow -E$ symmetry and the $N/2$ states at negative energy are doubly occupied and all other states are empty [see Fig. 7(b)], so that the sum over α in (32) should be restricted to $\alpha = 1, \dots, N/2$ such that $N = \sum_{\alpha=1}^{N/2} g$. In-gap edge states are at energy $\pm\Delta = \pm M \cos \theta$ and only exist when $\pi < \theta < 2\pi$. When in-gap edge states are at zero energy they are also called mid-gap edge states. A particular situation occurs when $\theta = 3\pi/2$ because there are two states that are almost degenerate at zero energy (actually there is a small energy splitting $\sim e^{-\#L}$ due to the finite size of the chain and the exponential overlap of the two edge states that leads to tunneling).

The resulting polarization is plotted in Fig. 5(b). It is not π but 2π -periodic with θ and does not remain between $-g/4$ and $g/4$. This is due to the appearance of two edge states when $\pi < \theta < 2\pi$. If we arbitrarily impose a modulo P_q , then we recover a result very close to the bulk polarization [see the pink crosses in Fig. 5(b)], with almost no finite-size effects (the two results differ by at most $3.10^{-3}P_q$ in absolute value when $N = 100$). Note that the strict Fermi-Dirac electronic filling that we use is not very physical when there are two edge states. Indeed, electrostatic interaction would favor having a single electron in each edge state (one on the left and one on the right) and not the two electrons occupying the same edge state as we assumed. The large jump in the polarization at $\theta = 3\pi/2$ is due to this filling. Indeed, it forces two electrons to suddenly change from one edge to the other as θ crosses $3\pi/2$, i.e. a charge $-g$ moves a distance L resulting in a polarization change of $\Delta P_{\text{open}} = (gL)/L = 2P_q$. If we adopt an alternative, more physical, filling [32] of edge states (i.e. one electron in each edge state, which are then half-filled), we recover a polarization that is almost identical to the odd case in the range $\pi < \theta < 2\pi$ [see the black points in Fig. 5(b) and compare with the green points in Fig. 5(a)]. In this way, we get rid of the large polarizations with $|P_{\text{open}}| > g/4$ and of the $2P_q$ jump at $\theta = 3\pi/2$. The polarization for the even open chain is then closer to that of the odd chain and converges towards the bulk result

in the thermodynamic limit.

D. Summary

In the thermodynamic limit, P_{open} (taken modulo P_q) tends towards P and not towards P_{cell} , eventhough both P_{open} and P_{cell} are obtained from the charge density, whereas P is obtained from the Zak phase. This shows the correctness of the Zak phase formulation of the bulk electric polarization [5, 6].

In summary, we agree with Ref. [5, 7, 21] on everything about the bulk electric polarization of the RM model except for the polarization quantum, which we find to be twice smaller: $P_q = g/2$ where $g = 1(2)$ for spinless (spinful) electrons. One consequence is that SSH has a vanishing bulk polarization and that it is best described as a molecular insulator (the molecules being non-polar dimers), despite its Wannier centers sitting mid-bond, i.e. $\langle x_- \rangle = 0$ or $1/2$ (when $\bar{x} = 0$). This factor of 2 in the polarization quantum is important for SSH as it agrees with the fact that the two dimerizations are identical and can not be distinguished in the bulk. Another consequence is that CDW has a quantized polarization $P_q/2$ and should be described as an ionic insulator (like a 1D version of rock salt $\text{Na}^+ \text{Cl}^-$), despite its Wannier centers sitting on the ions, i.e. $\langle x_- \rangle = \pm 1/4$ (when $\bar{x} = 0$).

IV. CHARGE ACCUMULATION AT DEFECTS

In this section, we discuss a relation between bulk electric polarization and charges that accumulate either at the edges of a finite system or at an interface between two domains. We discuss in particular the inversion-symmetric limits of the RM model, i.e. SSH and CDW.

A. Surface charge theorem

The prediction from the modern theory of polarization is that the end charge Q of a long open chain that is neutral and insulating obeys [5, 19, 33]:

$$Q = P + mP_q, \text{ with } m \text{ integer.} \quad (32)$$

This is a remarkable property, because it means that, independently of the surface termination, the end charge is constrained to take values set by the bulk only, in the sense that both P and P_q are fixed by the bulk, but the value of the integer m in Eq. (32) depends on the specific surface termination. In the above relation, P/P_q appears as the fractional part of the end charge (in units of P_q), while m appears as its integer part. This integer was recently discussed in [34]. It is worth mentioning at this point (see the discussion below) that jumps ΔQ in the end charge are always integers. This means that Δm can not take any integer value but must be such that:

$$\Delta Q = \Delta m P_q \in \mathbb{Z}. \quad (33)$$

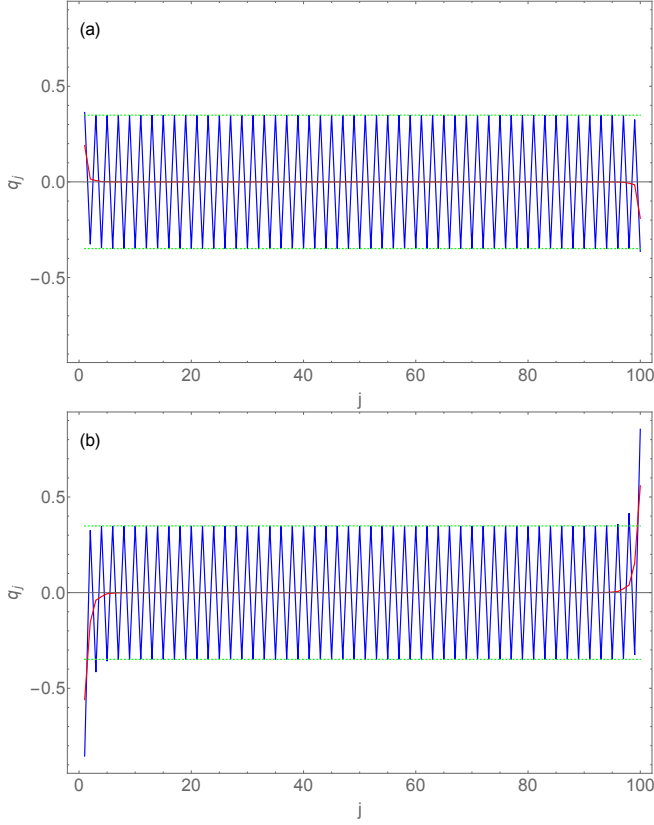


FIG. 8. Local charge as a function of site number $j = 1, \dots, N$ in an open chain with $N = 100$ sites for the spinful RM model with $M = 0.6$ and θ equal either to 0.2π or 1.2π . Blue is the charge q_j and red the smoothed charge \bar{q}_j . For comparison, the charge in the periodic case $q_j^0 \simeq \pm 0.348$ is shown as a green dashed lines, see Eq. (44). The end charge $Q = \sum_{j>N/2} \bar{q}_j$. (a) $\theta = 0.2\pi$ (no edge state), $Q(0.2\pi) \simeq -0.216$. (b) $\theta = 1.2\pi$ (one edge state per edge), $Q(1.2\pi) \simeq 0.784 = 1 + Q(0.2\pi)$.

In order to verify the above relation for the RM chain, we introduce the total charge of the chain

$$Q_{\text{tot}} = \int dx \rho(x) = \sum_{j=1}^N q_j = 0, \quad (34)$$

where the charge density is

$$\rho(x) = \sum_{j=1}^N q_j \delta(x - x_j) \text{ with } q_j = -g \sum_{\alpha \text{ occ.}} |\psi_\alpha(x_j)|^2 + \frac{g}{2}, \quad (35)$$

being the charge at site j . The smoothed charge density is defined as

$$\bar{\rho}(x) = \sum_{j=1}^N \bar{q}_j \delta(x - x_j) \quad (36)$$

with

$$\bar{q}_j = \frac{1}{2}q_j + \frac{1}{4}q_{j+1} + \frac{1}{4}q_{j-1} \text{ for } 1 < j < N \quad (37)$$

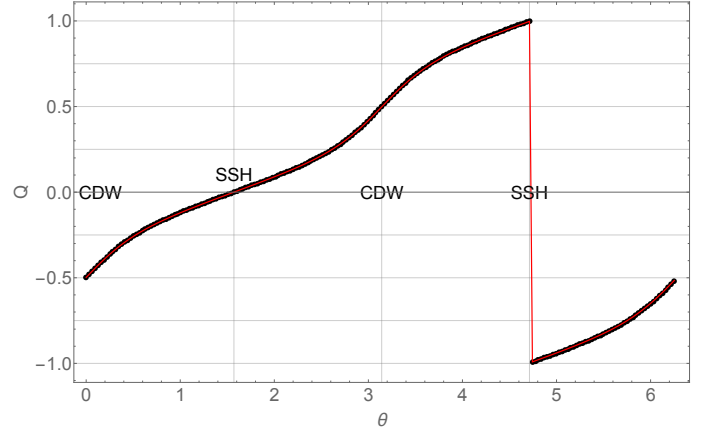


FIG. 9. End charge Q computed from the smoothed charge density as a function of θ for an open chain of the spinful RM model with $M = 0.6$ with 100 sites (in black). For comparison, $P_{\text{open}} = Q_{\text{eff}}$ is also plotted (red line).

and

$$\bar{q}_1 = \frac{3}{4}q_1 + \frac{1}{4}q_2 \text{ and } \bar{q}_N = \frac{3}{4}q_N + \frac{1}{4}q_{N-1}, \quad (38)$$

for the first and last sites of the chain [35] (see Fig. 8).

Next, we separate the chain into two “surfaces” (or ends) and a bulk [see Fig. 10(a)]. By definition, the bulk of the chain contains an integer number of unit cells and is extensive. The two surfaces are not extensive, but otherwise are arbitrary and can have different kind of terminations. The end charge Q is obtained by integrating the smoothed charge density near one end of the chain (we choose the right end, the left end having an opposite charge $-Q$).

We have probed numerically the correctness of the relation (32) by checking that

$$|\text{mod}(Q, P_q)| = P, \quad (39)$$

where P is given in Eq. (24) and $\text{mod}(x, x_0)$ means that x is taken modulo x_0 such that $-x_0/2 \leq \text{mod}(x, x_0) < x_0/2$. The end charge Q is also found to agree with the polarization computed for the same open chain $P_{\text{open}} = Q_{\text{eff}}$ (see Fig. 9).

A surface charge is not necessarily associated to the existence of an in-gap edge state (or even more restrictively to that of a mid-gap edge state). For example, for an open even chain, there is a surface charge when $0 < \theta < \pi$ [see Fig. 5(b)] but no in-gap edge states [see Fig. 7(b)]. The reason is that some of the bulk states are able to accumulate charges on one end of the chain without being exponentially localized near that edge. We have sorted eigenstates $|\psi_\alpha\rangle$ states according to whether their average position $\langle x_j \rangle_\alpha$ is larger or smaller than $L/2$ (see the bulk states plotted in red or blue in Fig. 7). Typically these are states at the edge of the bulk band gap. They are similar to that found for a 1D particle in an interval of length L with eigenvalue equation

$-\partial_x^2\psi(x) = E\psi(x)$ and mixed boundary conditions such that $\psi(0) = 0$ and $\partial_x\psi(L) = 0$. Such bulk states have a node at $x = 0$ and an anti-node at $x = L$ so that they have much more weight on the right edge. This effect is much more pronounced when N is odd then even, in Fig. 7 compare (a) with (b). When summing over all eigenstates $\sum_\alpha \langle x_j \rangle_\alpha = L/2$. This explains the red and blue pattern observed in valence and conduction bands as a compensation of the edge states.

Such a bulk-boundary correspondence (32) between bulk polarization and boundary charge is valid for any 1D band insulator and does not depend on the fact that the bulk can be separated into different topological classes or not. In the next section, we discuss what happens when inversion symmetry is further imposed.

B. Bulk-boundary correspondence for inversion-symmetric insulators

For chains that are centro-symmetric in the bulk (but the surface does not have to respect inversion symmetry), the bulk polarization $P = 0$ or $P_q/2$ modulo P_q so that Eq. (32) becomes

$$Q = \text{integer } P_q/2, \quad (40)$$

a result known since Heine in 1966 [36] (for review, see [33]). Equation (40) is slightly misleading as it does not distinguish between the two kinds of inversion-symmetric insulators. For example, for the SSH chain, as $P = 0$ modulo P_q , it means that $Q = \text{integer } P_q$, while for CDW, as $P = P_q/2$ modulo P_q , it means that $Q = (\text{integer} + 1/2)P_q$. In the spinless case, it is then predicted that SSH can only have end charges that are integer multiple of $P_q = 1/2$. This is the celebrated fractional charge discovered by Jackiw and Rebbi [37]. In the spinful case, the end charges are multiple integers of $P_q = 1$, as found by [18].

Playing with difference terminations for finite open chains, we have verified numerically that the end charge Q always satisfies the above relation as long as the Fermi level is in the bulk gap and the system is insulating. Figures 10 (CDW) and 11 (SSH) show inversion-symmetric examples of an open chain of the spinful RM model with $N = 101$ sites as a function of an edge potential V_b . The open chain is made asymmetric on purpose by deciding that the left most site has on-site energy $-V_b$ and the four rightmost sites have on-site energy $+V_b$. All other on-site energies follow the RM model and all hopping amplitudes as well. In these Figures, the energy spectrum is also shown (in black) and the levels that reside on the left (resp. right) edge are plotted in red (resp. blue). We observe that the end charge Q is very well quantized as long as the Fermi level lies in the bulk gap.

We also observe that jumps ΔQ in the end charge, see Eq. (33), correspond to level crossing between edge states living on opposite edges. Here, jumps ΔQ are in integer multiples of 1 (and not of 2), because we have chosen a

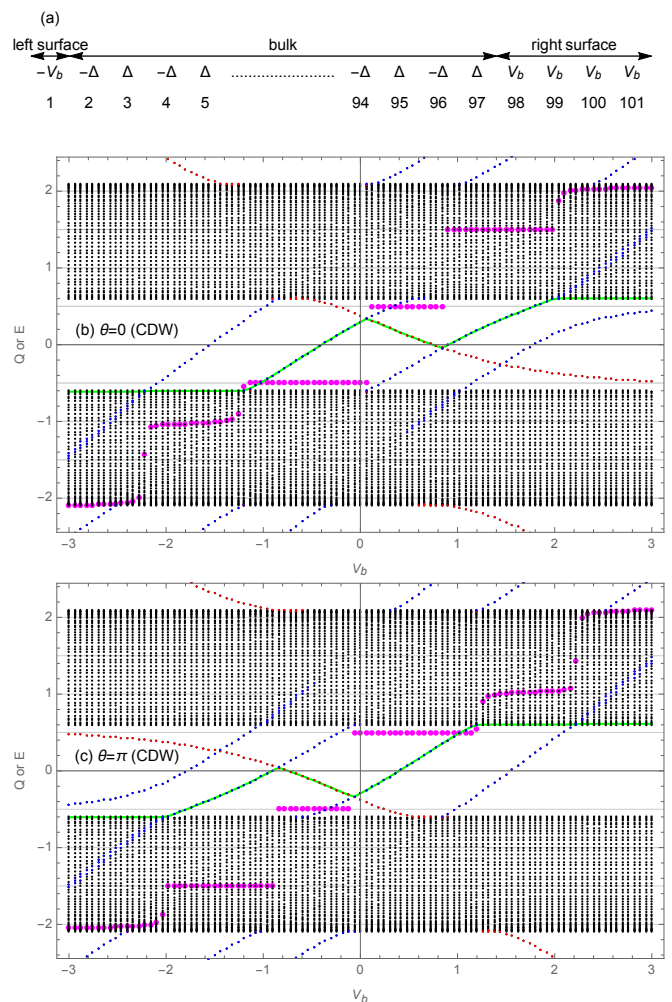


FIG. 10. (a) Sketch of an open spinful CDW chain with $M = 0.6$ and 101 sites and an asymmetric surface termination tuned by V_b . (b,c) End charge Q (magenta) and energy spectrum E (in black) as a function of V_b . Red (blue) indicates states localized on the left (right) edge of the chain. The green line indicates the last occupied state (Fermi level). When the Fermi level is inside the gap, each jump $\Delta Q = 1$ of the end charge Q corresponds to an energy level crossing of two edge states. (b) $\theta = 0$ ($\Delta > 0$), (c) $\theta = \pi$ ($\Delta < 0$). Here, $P_q = g/2 = 1$.

chain with an odd number of sites so that the last occupied level contains a single electron (i.e., is half-filled). For an even chain, with standard Fermi-Dirac filling, only fully occupied or fully empty levels are present and jumps are in units of 2. However, a more physical filling – allowing several partially filled levels – shows jumps in units of 1.

Steps in the end charge are always integer multiples of $\Delta Q = g$ because the smallest charge step corresponds to a single electron that jumps from one side to the other of the open chain. However, the absolute value of the end charge can reveal the polarization quantum. The

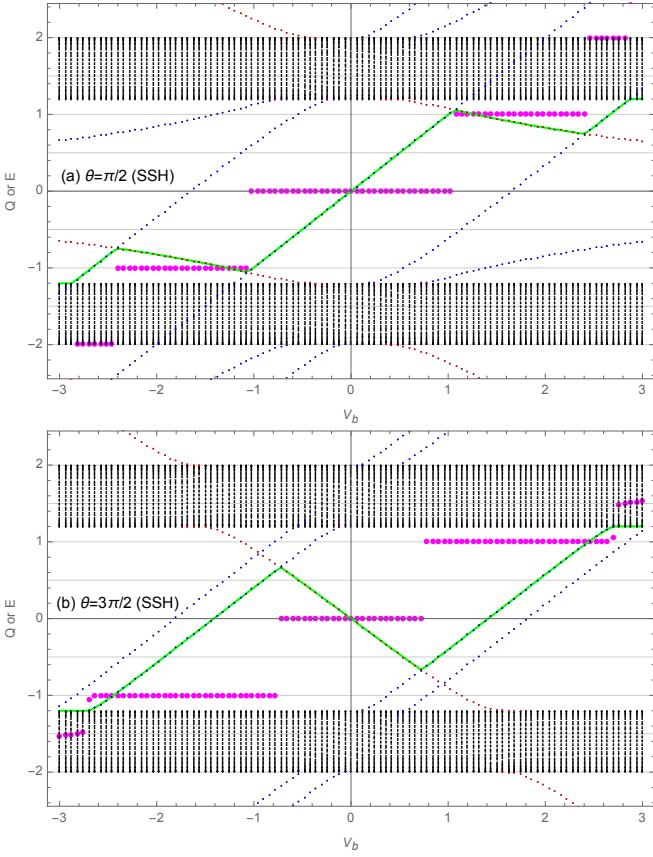


FIG. 11. Same as in Fig. 10 but for an odd SSH chain with 101 sites. (a) $\theta = \pi/2$ ($\delta > 0$), (b) $\theta = 3\pi/2$ ($\delta < 0$). Here, $P_q = g/2 = 1$.

polarization quantum only depends on the Bravais lattice and on the charges of the crystal's constituents (ions and electrons) but it does not depend on the parameters of the electronic Hamiltonian. It is therefore the same for any value of δ and Δ (or M and θ) in the RM model. By playing with the Hamiltonian parameters and probing the end charge for different lattice terminations, one can infer the polarization quantum. Indeed, when inversion symmetry is present the polarization P is either 0 or $P_q/2$. In that case, if the minimal end charge $Q_{\min} = 0$, then one can conclude that $P = 0$ and that $P_q = \Delta Q / \text{integer} \leq g$, which gives an upper bound but not the precise value of P_q . But if $Q_{\min} \neq 0$, then the polarization quantum is:

$$P_q = 2|Q_{\min}| > 0. \quad (41)$$

From Fig. 11, we see that $Q_{\min} = 0$ and $\Delta Q = 1$ so that $P = 0$ and $P_q = 1/\text{integer} \leq 1$. Already at this point, $P_q = 2$ is no longer a possibility. From Fig. 10, we see that $Q_{\min} = 1/2$ and therefore that $P = 1/2$ and $P_q = 1 = g/2$.

An important conclusion is that the polarization quantum is a physical quantity that can be measured in princi-

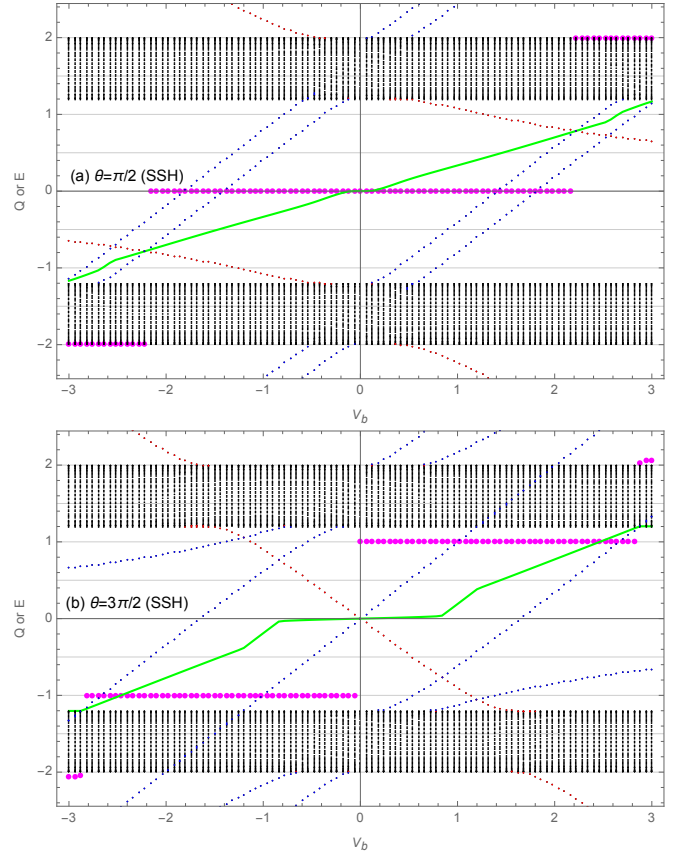


FIG. 12. Same as Fig. 11 but for an even SSH chain with 100 sites.

ple from the end charges. It is therefore not a convention or a choice.

Figs. 11 and 12 illustrate the even/odd effect on the SSH chain. In particular, it is tempting, but wrong, to interpret Fig. 12(b) as corresponding to a topological phase with quantized polarization $P = 1$.

The bulk-boundary correspondence for inversion-symmetric insulators is in terms of quantized end charges and not in terms of in-gap edge states: for trivial insulators $Q = 0 [P_q]$ and for topological insulators $Q = P_q/2 [P_q]$. As we have seen, edge states are not required in order to have end charges (see also the discussion in [34]). In addition, this form of bulk-edge correspondence does not require that the protecting symmetry (here inversion symmetry) is respected by the edges.

In the end, in the thermodynamic limit, the bulk polarization P , the open chain polarization $P_{\text{open}} = Q_{\text{eff}}$ and the end charge Q all agree modulo P_q .

C. Interface theorem: soliton charge

Just like an edge, a domain wall or interface between two band insulators a and b can also be charged. This is known as the interface or soliton charge Q_{sol} . The

prediction in that case is that [5, 33]:

$$Q_{\text{sol}} = P_a - P_b + mP_q \text{ with } m \text{ integer.} \quad (42)$$

The interface charge is defined from the charge density as

$$Q_{\text{sol}} = \sum_{j=j_b}^{j_a} (q_j - q_j^0), \quad (43)$$

where the site j_b is much before the domain wall at j_0 and the site j_a is much after (typically $j_a - j_0 \sim j_0 - j_b \geq 10$), q_j is the charge at site j in the presence of the domain wall and q_j^0 the charge at j when there is no domain wall (i.e. the periodic chain). The latter can be computed analytically in the thermodynamic limit

$$\begin{aligned} q_j^0 &= -g \int_{-\pi}^{\pi} \frac{dk}{2\pi} |u_{-,k}(x_j)|^2 + \frac{g}{2} \\ &= \pm \frac{g}{2} \frac{\Delta}{\pi \sqrt{1 + \Delta^2/4}} K\left(\frac{1 - \delta^2}{1 + \Delta^2/4}\right), \end{aligned} \quad (44)$$

where \pm refers to sites $j = A$ or B . This calculation is similar to that leading to Eq. (30), see Appendix A.

In particular, in the RM model, if the domain wall is due entirely to a mismatch in the dimerization δ (as in the SSH case), then Eq. 42 gives

$$\begin{aligned} Q_{\text{sol}} &= P(\Delta, \delta) - P(\Delta, -\delta) = 2P(\Delta, \delta) \\ &= -\frac{g}{\pi} \frac{\Delta \delta}{2\sqrt{1 + \Delta^2/4}} \Pi\left(1 - \delta^2, \frac{1 - \delta^2}{1 + \Delta^2/4}\right), \end{aligned} \quad (45)$$

where all equalities are taken modulo P_q . In the limit $|\delta|$ and $|\Delta| \ll 1$, we can use Eq. (25) to obtain:

$$Q_{\text{sol}} \simeq -\frac{g}{\pi} \arctan \frac{\Delta}{2\delta}. \quad (46)$$

In this form, we recognize the irrational charge Q_0 predicted by Rice and Mele for spin 0 solitons [10]. For a nice derivation of the arctan result from a general perspective and using the Dirac equation, see Stone [38]. Fundamentally, this result is related to the Friedel sum rule.

We have checked the general relation (45) numerically for finite chains with PBC and two such domain walls (one soliton and one anti-soliton). In practice, we have computed the interface charge Q_{sol} from the charge density near one domain wall and checked that

$$|\text{mod}(Q_{\text{sol}}, P_q)| = |\text{mod}(2P, P_q)|, \quad (47)$$

where P is given in Eq. (24) and the modulo is defined as in Eq. (39). The analytical formula (45) is therefore a generalization of the irrational soliton charge found by Rice and Mele but valid at arbitrary energy and not restricted to $|\Delta|, |\delta| \ll 1$.

In the particular case where there is inversion symmetry, $Q_{\text{sol}} = \text{integer } P_q$. In the spinless case, this gives the famous result of the fractional soliton charge $Q_{\text{sol}} = \text{integer } \frac{1}{2}$ found by Jackiw and Rebbi [37] and by SSH [18]. In this case the domain wall is a true topological defect, whereas for the general RM model, a domain wall is a topological texture.

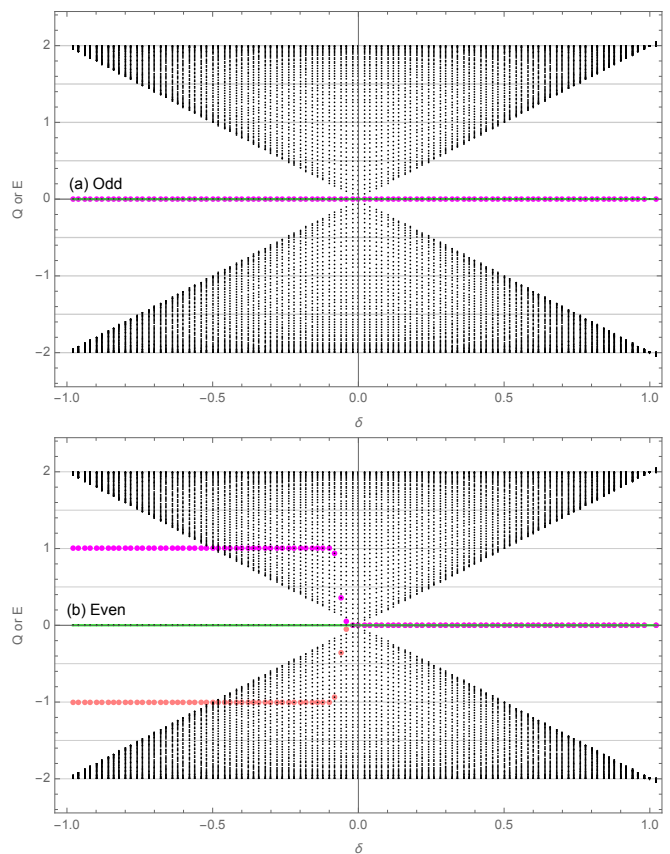


FIG. 13. Phase transition in an open spinful SSH chain with (a) 101 or (b) 100 sites. The energy E (black) and the end charge Q (magenta and pink) are plotted as a function of the control parameter δ . The Fermi level is in green. Here, $P_q = g/2 = 1$.

D. Gap-closing phase transition in SSH and CDW

We now consider a gap-closing phase transition either in the spinful SSH or CDW chain. In the first case, the transition is controlled by the dimerization δ and in the second by the staggered on-site potential Δ . In Figs. 13 and 14, we monitor the energy spectrum and the end charge of a spinful open chain as a function of the control parameter. The purpose is to infer the bulk polarization from the end charge.

For the odd SSH chain [see Fig. 13(a)], inversion symmetry is absent globally and there is always a single zero energy edge state, which is occupied by a single electron (all other states are either doubly occupied or empty), so that there is no difference between $\delta > 0$ and $\delta < 0$ and $Q = 0$ always. For the even chain [see Fig. 13(b)], inversion symmetry is present globally, so that the end charge should always vanish in principle. When $\delta > 0$, Q is indeed 0. However, when $\delta < 0$, $Q = 1$. This comes from the near degeneracy of the two mid-gap edge states. In the thermodynamic limit, the tunnel splitting vanishes and there is the possibility of spontaneous sym-

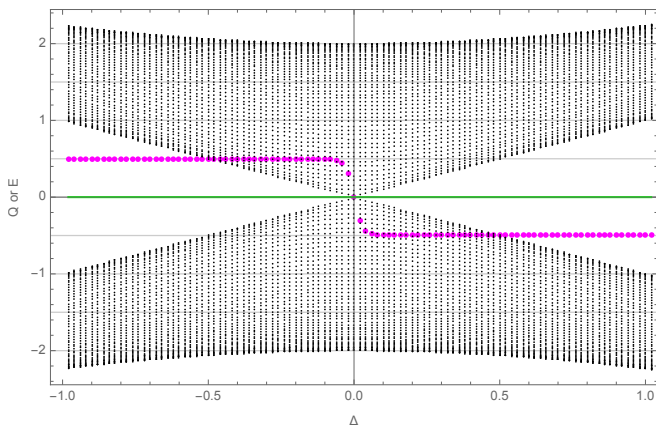


FIG. 14. Phase transition in an open spinful CDW chain with 100 sites. The energy E (black) and the end charge Q (magenta) are plotted as a function of the control parameter Δ . The Fermi level is in green. Here, $P_q = g/2 = 1$.

metry breaking. Numerically, we help the latter by explicitly breaking the global inversion symmetry with an infinitesimal staggered on-site potential on the two end sites $\pm\eta$ with $|\eta| \sim 10^{-3}$. With $\eta > 0$, this gives $Q = 1$ (shown in magenta), while $\eta < 0$ gives $Q = -1$ (shown in pink). If $\eta = 0$, then the global inversion symmetry forces $Q = 0$ also for $\delta < 0$ (this requires increasing the numerical precision such as to resolve the exponentially small tunneling splitting between the two mid-gap states). It is therefore a finite-size effect. In addition, the comparison between even and odd chains in Fig. 13 shows that $P_q = 1$. Therefore, the bulk polarization $P = 0 \bmod P_q$ for both dimerizations. The conclusion is that, in the bulk, the two sides of the transition (i.e. the two dimerizations) correspond to a single trivial phase.

In the CDW chain, the even chain breaks global inversion symmetry such that $Q = \pm 1/2$ (see Fig. 14), which clearly shows that the bulk polarization is $P = P_q/2 \bmod P_q = 1$ for both signs of Δ . The odd chain can not be studied because it can not be both electrically-neutral and insulating. In the bulk, the two sides of the transition therefore correspond to a single topological phase.

Note that, in the bulk at the gap-closing transition, the inversion symmetry is of mixed type and is therefore different from the inversion symmetry in the gapped phases (bond inversion for SSH, site inversion for CDW). It is possible to build a toy model from the inversion-symmetric RM that realizes a true phase transition between $P = 0$ and $P = P_q/2$, see [39]. This requires tuning a transition from SSH to CDW.

V. SHOCKLEY MODEL

The Shockley model of coupled s and p bands [5, 9] is sometimes assumed to be identical to the SSH model, see e.g. [40, 41]. Here, we wish to show that it is actually

different, although closely related. In some sense, it is a simpler example of an inversion-symmetric insulator, which contains both phases (vanishing or quantized polarization) and avoids some of the subtleties of the RM model. In particular, there is a unique Bloch Hamiltonian.

A. Generic case

Here, we follow the analysis of Vanderbilt and King-Smith [5]. The Shockley model is a 1D tight-binding model with a single site per unit cell but two orbitals (s and p) per site. The s orbital is even under inversion, while the p orbital is odd. Here the polarization quantum is $P_q = g$ if the lattice spacing $a = 1$, the electron charge is -1 (g electrons per unit cell) and the ion charge is $+g$. The factor of 2 difference with RM for the polarization quantum comes from having a single ion of charge $+g$ instead of two ions of charge $+g/2$.

The Bloch Hamiltonian is

$$H(k) = \left[\frac{\epsilon_s + \epsilon_p}{2} + (t_{ss} + t_{pp}) \cos k \right] \sigma_0 \quad (48)$$

$$+ \left[\frac{\epsilon_s - \epsilon_p}{2} + (t_{ss} - t_{pp}) \cos k \right] \sigma_z + 2t_{sp} \sin k \sigma_y,$$

where $t_{ss} \leq 0$, $t_{pp} \geq 0$ and t_{sp} are hopping amplitudes and $\epsilon_s \leq 0$ and $\epsilon_p \geq 0$ are orbital energies. Inversion symmetry acts as $\sigma_z H(-k) \sigma_z = H(k)$ and is of mixed type: one inversion center is on-site and the other is mid-bond.

When $\epsilon_p - \epsilon_s > 2(t_{pp} - t_{ss})$, the Wannier center is on-site so that the polarization vanishes. It describes an atomic insulator with s -type valence band and p -type conduction band.

A band inversion occurs at $\epsilon_p - \epsilon_s = 2(t_{pp} - t_{ss})$ and the gap closes.

When $\epsilon_p - \epsilon_s < 2(t_{pp} - t_{ss})$, the Wannier center is mid-bond and the polarization is quantized to $P_q/2$. It is a covalent insulator with a valence (resp. conduction) band of bonding (resp. anti-bonding) hybridized sp -type.

As it has a simple Bravais lattice (no basis), the canonical Bloch Hamiltonian is periodic $H(k + 2\pi) = H(k)$ and there is no difference between canonical and periodic Bloch Hamiltonians (see Appendix B).

For a generic choice of parameter, the Shockley model does not have a chiral symmetry, belongs to the AI class and should therefore be a trivial insulator according to the ten-fold way periodic table [11–13]. But it still has its \mathbb{Z}_2 classification as an inversion-symmetric insulator: vanishing polarization if $\epsilon_p - \epsilon_s > 2(t_{pp} - t_{ss})$ and quantized polarization if $\epsilon_p - \epsilon_s < 2(t_{pp} - t_{ss})$. As such, it fits into the family of topological crystalline insulators, protected by inversion symmetry.

B. Chiral symmetry

For a specific choice of parameters ($\epsilon_s = -\epsilon_p$ and $t_{ss} = -t_{pp}$), the Bloch Hamiltonian simplifies to:

$$H(k) = -(\epsilon_p + 2t_{pp} \cos k)\sigma_z + 2t_{sp} \sin k \sigma_y. \quad (49)$$

In addition to time-reversal symmetry, the model now possesses a chiral symmetry as $\{H(k), \sigma_x\} = 0$ (here of “internal type” and not related to sublattices) and belongs to the BDI class in 1D [11–13]. It is therefore characterized by a bulk winding number, which is $W = \text{sign } t_{sp}$ if $\epsilon_p < 2t_{pp}$ (covalent insulator) and $W = 0$ if $\epsilon_p > 2t_{pp}$ (atomic insulator). The latter is here a measurable quantity related to the electric polarization by:

$$P = g \frac{W}{2} \text{ modulo } g. \quad (50)$$

For the polarization, the winding number only matters modulo 2. This is how the \mathbb{Z} classification for chiral insulators becomes a \mathbb{Z}_2 classification for inversion-symmetric insulators. The above restricted Shockley model is a simple example of chiral insulator.

The Bloch Hamiltonian (49) of the chiral Shockley model can be mapped onto the periodic Bloch Hamiltonian (B1) of the SSH model, see Appendix B, by

$$\begin{aligned} t_{sp} = t_{pp} &\rightarrow -w/2 \\ \epsilon_p &\rightarrow -v \\ (\sigma_x, \sigma_y, \sigma_z) &\rightarrow (-\sigma_z, \sigma_y, \sigma_x) \end{aligned} \quad (51)$$

The two models have essentially the same tight-binding Hamiltonian (same connectivity between orbitals, same real-space topology) but the orbitals do not have the same spatial embedding (i.e. not the same real-space geometry) and hence the position operators are different. The models are therefore different, the key difference being that the two orbitals in the Shockley model belong to the same site (the same ion), whereas in the SSH model they belong to two different ions. For example, when $\epsilon_p = -v > 2t_{pp} = -w$, the electric polarization vanishes in the Shockley model and in the SSH model. However, when $\epsilon_p = -v < 2t_{pp} = -w$, it becomes quantized ($P = P_q/2 = g/2$ modulo g) in the Shockley model but vanishes ($P = 0$ modulo $g/2$) in SSH.

In the following, for simplicity (i.e. in order to reduce the number of parameters), we restrict to the chiral Shockley model. However, we have checked that chiral symmetry plays no crucial role in all of the following results, which are a consequence of inversion symmetry.

C. Surface charge

We now study how the surface charge of an open chain of the spinful chiral Shockley model depends on a surface potential V_b similarly to what we have done for RM. The surface potential is $-V_b$ on the first orbital on the left surface and is $+V_b$ on the four last orbitals on the right

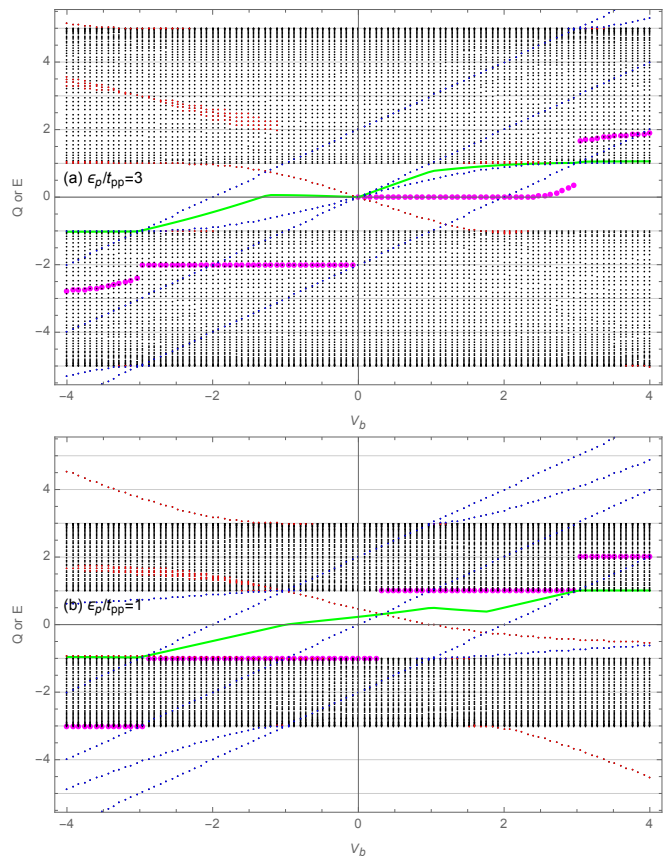


FIG. 15. Open chain of the spinful chiral Shockley model with 50 sites (and 100 orbitals). End charge Q (magenta) and energy spectrum E (in black) as a function of V_b . Red (blue) indicates states localized on the left (right) edge of the chain. The green line indicates the last occupied state (Fermi level). When the Fermi level is inside the gap, each jump $\Delta Q = 2$ of the end charge Q corresponds to an energy level crossing of two edge states. (a) $\epsilon_p/t_{pp} = 3$, (b) $\epsilon_p/t_{pp} = 1$. Here, $P_q = g = 2$.

surface, similarly to Fig. 10(a). In Fig. 15, we see that the end charge is quantized when the Fermi energy is in the bulk gap and that Q jumps by multiples of $\Delta Q = 2$. This is due to the fact that every level is either doubly occupied ($g = 2$) or empty. Therefore, when an electron pair jumps from one side of the chain to the other, the end charge changes by 2.

We also find two different behaviors when $\epsilon_p > 2t_{pp}$ or $\epsilon_p < 2t_{pp}$. On the one hand, from Fig. 15(a), when $\epsilon_p > 2t_{pp}$, we see that $Q_{\min} = 0$ so that $P = 0$, which corresponds to a trivial phase, and the polarisation quantum can only take one of the following values $P_q = 2/\text{integer} \leq 2$. On the other hand, when $\epsilon_p < 2t_{pp}$, we see in Fig. 15(b) that $Q_{\min} = 1$ so that $P_q = 2 = g$ and therefore $P = 1 \text{ mod } 2$, corresponding to a topological phase. In this regime, there are two mid-gap edge states (one per edge), following the mechanism discovered by Shockley [9].

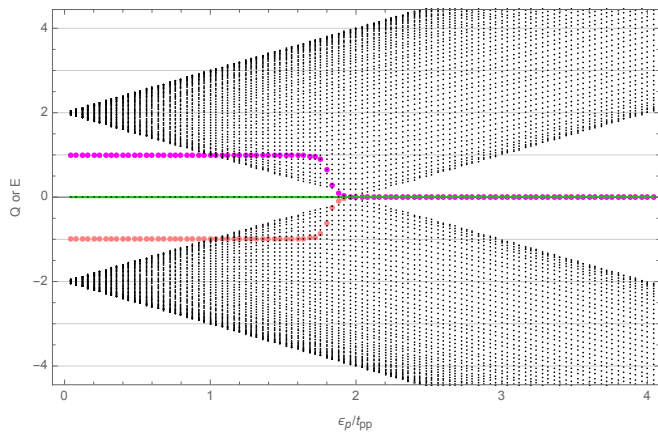


FIG. 16. Phase transition in an open chain of the spinful chiral Shockley model with 50 sites. The energy E (black) and the end charge Q (magenta and pink) are plotted as a function of the control parameter ϵ_p/t_{pp} . The Fermi level is in green. Here, $P_q = g = 2$.

D. Gap-closing phase transition

We now consider the gap-closing phase transition in the chiral Shockley chain. The transition is controlled by the parameter ϵ_p/t_{pp} . In Fig. 16, we monitor the energy spectrum and the end charge Q of a spinful open chain in order to infer the bulk polarization. For the Shockley chain, there is no even/odd effect. For any N , the open chain has a global inversion symmetry and in principle one expects $Q = 0$. Again, there is the possibility of spontaneous symmetry breaking in the regime where there are two mid-gap edge state that are degenerate in the thermodynamic limit. In the numerics, we add an infinitesimal staggered on-site potential $\pm\eta$ on the two end sites to break the global inversion symmetry. In Fig. 16, one has $Q = 1$ (in magenta) when $\eta > 0$ and $Q = -1$ (in pink) when $\eta < 0$.

We find that $Q = 0$ when $\epsilon_p/t_{pp} > 2$ and that $Q = 1$ when $\epsilon_p/t_{pp} < 2$. It means that the polarization $P = 0$ when $\epsilon_p/t_{pp} > 2$ and that $P = P_q/2 \bmod P_q = g = 2$ when $\epsilon_p/t_{pp} < 2$. In contrast to SSH and CDW, the two sides of the transition are truly different and correspond to distinct phases.

In the bulk, at the gap-closing transition, the inversion symmetry is of mixed type and is therefore identical to that in the two gapped phases. The phase transition is therefore truly topological and does not result from a change of symmetry. It is therefore different from the phase transitions in both SSH and CDW chains.

VI. ADIABATIC PUMPING

Thouless [42] has shown that there is a topological origin to the quantization of adiabatic transport in periodically-driven one-dimensional band insulators.

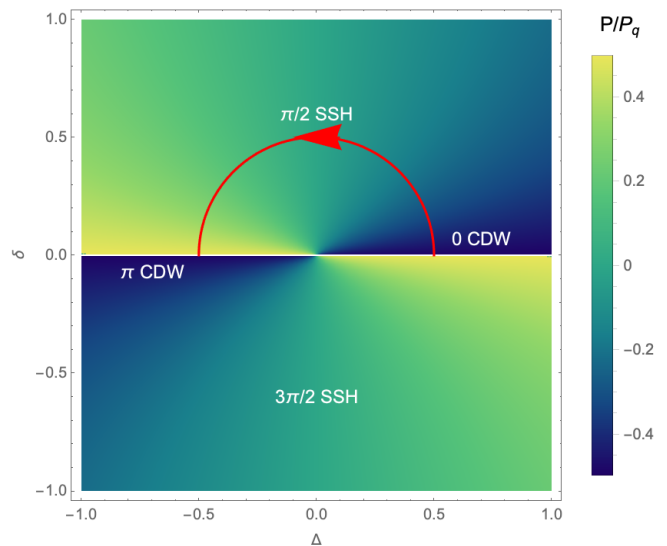


FIG. 17. Adiabatic pumping in the RM model. Bulk polarization P (in units of the polarization quantum $P_q = g/2$) in the (Δ, δ) plane. If the parameters Δ and δ are half-cycled between $\theta = 0$ and π , a charge g is displaced by a distance $1/2$. For a full cycle, a charge g is displaced by a unit distance. Compare with Fig. 2 in [7].

When parameters of the model are pumped (i.e. time-cycled), an integer number C of charges are adiabatically transported during each cycle. This C is the Chern number that characterizes the filled bands under periodic driving and which is computed in the effective Brillouin zone (k, t) , where t is the time that spans one period.

Here we consider the situation discussed by Xiao et al. [7] of adiabatic pumping in the spinless ($g = 1$) RM model. Our aim is to study the consequences of the unusual polarization quantum $P_q = g/2 = 1/2$ on adiabatic pumping.

The driving parameter is taken to be θ , so that the effective Brillouin zone is spanned by (k, θ) with $\Delta = M \cos \theta$ and $\delta = M \sin \theta$. The corresponding 2D Bloch Hamiltonian reads

$$H(k, \theta) = 2 \cos \frac{k}{2} \sigma_x + 2M \sin \theta \sin \frac{k}{2} \sigma_y + M \cos \theta \sigma_z, \quad (52)$$

which explicitly breaks 2D time-reversal symmetry $H(-k, -\theta)^* \neq H(k, \theta)$ but satisfies 2D inversion symmetry $H(-k, -\theta) = H(k, \theta)$. For a given band n , the Chern number C_n is related to the Zak phase $Z_n = \int_{-\pi}^{\pi} dk \langle u_n | i \partial_k u_n \rangle$ by:

$$\begin{aligned} C_n &= \frac{1}{2\pi} \int_0^{2\pi} d\theta \frac{dZ_n}{d\theta} \\ &= \frac{1}{2\pi} \int d\theta dk (\langle \partial_\theta u_n | i \partial_k u_n \rangle - \langle \partial_k u_n | i \partial_\theta u_n \rangle). \end{aligned} \quad (53)$$

Using the relation between the Zak phase and the polarization, for one full cycle, the Chern number of the

valence band is given by

$$C = - \int_{\theta_0}^{\theta_0+2\pi} d\theta \frac{dP}{d\theta} = -2P_q$$

$$\simeq \int_{\theta_0}^{\theta_0+2\pi} d\theta \frac{-2\pi}{2\pi(1+3\sin^2\theta)} = -1, \quad (54)$$

for any initial angle θ_0 . For simplicity, in the second equality, we have used the bulk polarization of Eq. (25), valid when $M \ll 1$, but the same result follows from integrating the exact formula with the elliptic function in Eq. (24). Actually, this integral does not depend on M .

The main differences with [7] are that the polarization quantum is twice smaller $P_q = 1/2$ and that the parameters of the RM model can be restricted to θ in $[0, \pi[$ (see Fig. 2 in [7] and compare with Fig. 17). Therefore quantized adiabatic transport should already occur for half a cycle, i.e. when the parameter θ increases by π (and not 2π). Indeed, we have seen that $P(\theta)$ is π -periodic and therefore $\frac{dP}{d\theta}$ is also π -periodic. As a consequence, there is already an exact quantization for half a cycle

$$- \int_{\theta_0}^{\theta_0+\pi} d\theta \frac{dP}{d\theta} = -P_q = -\frac{1}{2} = \frac{C}{2}, \quad (55)$$

for any θ_0 . In such a process, in each unit cell, a unit charge is displaced by a distance $1/2$. The meaning of this $1/2$ is therefore *not* that of a fractional charge $1/2$ that would be displaced by a unit distance. The fact that the charge transported during the first half-cycle is exactly the same as that transported during the second half-cycle was already noted for 1D particle-hole-symmetric insulators in [17]. It reflects the fact that a 2D version of the symmetry (either inversion or particle-hole) is satisfied.

Imagine a semi-infinite RM chain (along the negative x axis) that is pumped in order to transport charges from left to right, and say that the conveyor belt initially follows the charge pattern-1-0-1-0-1-0 as shown in Fig. 18(Top). Consider, e.g., that the initial state is CDW ($\theta_0 = \pi$). There is only one Wannier center per unit cell but two sites, so that only one site out of two is occupied by an electron (A is occupied but B is empty). Therefore, at the right end $x = 0$ of the semi-infinite chain, after pumping for half a cycle (θ from θ_0 to $\theta_0 + \pi$), no charge comes out. But every electron has moved by a distance $1/2$ to the right. Now the charge pattern looks like0-1-0-1-0-1 [see Fig. 18(Middle)], so that during the next half-cycle (θ from $\theta_0 + \pi$ to $\theta_0 + 2\pi$), exactly one unit charge comes out of the chain at the right end [see Fig. 18(Bottom)]. And this occurs in systematic alternation. Each half-cycle moves a unit charge by a distance $1/2$, but in order to transport a unit charge over a unit distance (unit cell) one needs a full cycle.

Actually, such an effect has already been measured [43, 44] but remained unnoticed. In Fig. 2 of [43] (see also Fig. S3 of the supplementary material of [44]), it is apparent that the quantization of adiabatic transport in the

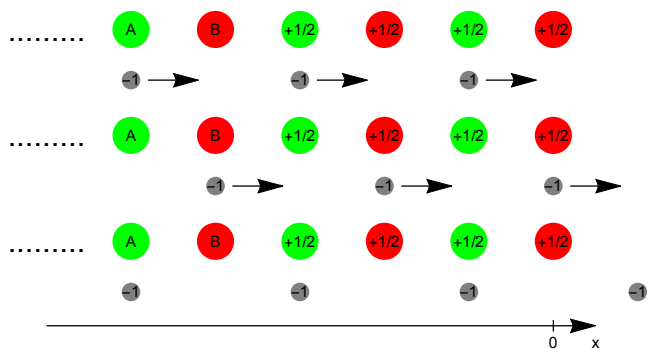


FIG. 18. Adiabatic pumping in a spinless RM chain starting from a CDW state in which the Wannier center is on an A site ($\theta_0 = \pi$). (Top) First half-cycle (θ between θ_0 and $\theta_0 + \pi$). (Middle) Second half-cycle (θ between $\theta_0 + \pi$ and $\theta_0 + 2\pi$). During half a cycle, each electron moves exactly by half a unit cell. (Bottom) At the end of a full cycle, a unit charge comes out of the right end of the chain.

RM chain already occurs for half-a-cycle. In these experiments, half-a-cycle induces a displacement of a distance $a/2$, where a is the size of the unit cell.

VII. CONCLUSION

The bulk electric polarization of a 1D periodic crystal is defined modulo a polarization quantum [5]. Therefore the polarization is best thought as being an angle $\vartheta = 2\pi P/P_q$ [16]. This is true quantum mechanically and classically.

The polarization quantum is a measurable quantity, as we have shown. It is not always given by $P_q = ge$, i.e. it not only depends on the electron charge but also on the charge of ions. However, it does not depend on the parameters of the electronic Hamiltonian such as hopping amplitudes, on-site potentials, etc.

Ions are crucial to maintain electro-neutrality, in order to obtain a well-defined polarization, and in determining the polarization quantum. However, it is not the charge *per se* which is essential but the fact that mobile particles (“electrons”) and the static lattice of sites (“ions”) are both taken into account. Indeed the only thing that matters for the bulk polarization is the relative position of the Wannier center with respect to the lattice. Our result therefore also applies to artificial realizations of the RM model or the SSH chain with “chargeless electrons” such as cold atoms in optical lattices [45], microwaves in lattices of dielectric resonators [46] or polaritons [47].

One-dimensional insulators without any symmetry only exist in a single class [11–13]. However, any symmetry (such as inversion) that acts on the polarization as $P \rightarrow -P$ creates two classes of insulators: one (trivial) with vanishing polarization and another (topological) with quantized polarization $P = P_q/2$ [15–17]. When in-

version symmetry is present, other symmetries such as chiral are irrelevant for this classification.

We have shown that inversion symmetry comes in three flavors: site inversion, bond inversion and mixed inversion. Two-band models that represent these three cases are CDW, SSH and Shockley. The first two happen to also have chiral symmetry, but this is an accident. It is easy to break chiral symmetry while preserving inversion symmetry and to see that the bulk polarization is unaffected.

The Shockley model has a single site per unit cell and its polarization quantum is the expected $P_q = g$. However, CDW and SSH (or more generally the RM model) have two sites per unit cell and their polarization quantum is half the expected value $P_q = g/2$. This is not a convention or a choice but is a measurable property. Our main results concerning these three models are summarized in Table I.

SSH is commonly taken as the simplest example of a topological insulator [13, 15, 22–28]. But does SSH really describe a bulk topological insulator? One important conclusion of our work is that SSH has a unique gapped phase with vanishing polarization (in agreement with [16, 19]), which makes it a trivial inversion-symmetric insulator.

As a chiral insulator, this question can not be answered as SSH does not have a well-defined bulk and absolute winding number (see Appendix B). This is due to the lattice with a basis that prevents the existence of a Bloch Hamiltonian that is both periodic with the first Brillouin zone and independent of a unit cell choice. Although SSH is neither an inversion-symmetric nor a chiral-symmetric topological insulator, it is an example of a Dirac insulator, with the property of trapping mid-gap states at domain walls [18, 37]. Our conclusion does not contradict the bulk-edge correspondence of chiral insulators in terms of an edge-dependent (relative) winding number related to the presence of mid-gap edge states [48–51].

In contrast, the Shockley model of coupled s and p bands is probably the simplest example of an inversion-symmetric insulator featuring both a trivial and a topological phase. In its chiral version, as the winding number is well-defined (because the canonical Bloch Hamiltonian is periodic), it is also a nice example of a chiral-symmetric insulator featuring a trivial and a topological phase.

In hindsight, the simple example of SSH shows that the ten-fold way classification of topological insulators and superconductors [11–13] relies on the existence of a periodic and well-defined Bloch Hamiltonian, which is not always possible when there is a lattice with a basis. As a perspective, it would be interesting to explore in higher space dimensions what are the modifications in these classifications in cases similar to SSH, i.e. lattices with a basis.

ACKNOWLEDGEMENTS

We thank János Asbóth, Jérôme Cayssol, Johannes Kellendonk, Andrej Mesáros and Julien Vidal for useful discussions.

Appendix A: Bulk electric polarization

In this appendix, we derive an analytical expression for the bulk electric polarization of the RM model (when $d = 1/2$). It reads

$$P = -\frac{g}{2\pi} Z_- + g\bar{x} \text{ modulo } P_q, \quad (\text{A1})$$

with

$$Z_- = \int_{-\pi}^{\pi} dk \langle u_- | i \partial_k u_- \rangle = \int_{-\pi}^{\pi} dk \frac{1 - \cos \theta_k}{2} \partial_k \phi_k \quad (\text{A2})$$

where

$$e^{i\phi_k} = \arg\left(\cos \frac{k}{2} + i\delta \sin \frac{k}{2}\right) \quad (\text{A3})$$

$$\text{and } \cos \theta_k = \frac{\Delta}{\sqrt{4 \cos^2 \frac{k}{2} + 4\delta^2 \sin^2 \frac{k}{2} + \Delta^2}}.$$

The two angles θ_k and ϕ_k define the position on the Bloch sphere of the cell-periodic Bloch state $|u_-(k)\rangle$, which is an eigenvector of the canonical Bloch Hamiltonian: $H(k)|u_-(k)\rangle = E_-(k)|u_-(k)\rangle$. When the position origin is such that $\bar{x} = -1/4$, the Zak phase reads

$$\begin{aligned} Z_- &= -\frac{\pi}{2} \text{sign } \delta \\ &+ \frac{\Delta\delta}{8} \int_{-\pi}^{\pi} \frac{dk}{(\cos^2 \frac{k}{2} + \delta^2 \sin^2 \frac{k}{2}) \sqrt{\cos^2 \frac{k}{2} + \delta^2 \sin^2 \frac{k}{2} + \Delta^2/4}} \\ &= -\frac{\pi}{2} \text{sign } \delta + \frac{\Delta\delta}{2\sqrt{1 + \Delta^2/4}} \Pi\left(1 - \delta^2, \frac{1 - \delta^2}{1 + \Delta^2/4}\right), \quad (\text{A4}) \end{aligned}$$

where $\Pi(n, m) = \int_0^{\pi/2} \frac{d\theta}{(1 - n \sin^2 \theta) \sqrt{1 - m \sin^2 \theta}}$ is the complete elliptic function of the third kind. As a function of M and θ , the bulk polarization reads:

$$\begin{aligned} P(M, \theta) &= -\frac{g}{4} \left[1 - \text{sgn} \sin \theta + \frac{M^2 \cos \theta \sin \theta}{\pi \sqrt{1 + M^2 \cos^2 \theta/4}} \times \right. \\ &\quad \left. \times \Pi\left(1 - M^2 \sin^2 \theta, \frac{1 - M^2 \sin^2 \theta}{1 + M^2 \cos^2 \theta/4}\right) \right]. \quad (\text{A5}) \end{aligned}$$

The (wrong) polarization calculated from the charge density can also be obtained analytically. From Eq. (28), it reads

$$P_{\text{cell}} = g\bar{x} - g \sum_{l=A,B} x_l \int \frac{dk}{2\pi} |u_{-,k}(x_l)|^2. \quad (\text{A6})$$

Using $|u_{-,k}(x_l)|^2 = \frac{1 \mp \cos \theta_k}{2}$, where $l = A$ or B , we obtain

$$\begin{aligned} P_{\text{cell}} &= -\frac{gd}{2} \int \frac{dk}{2\pi} \cos \theta_k \\ &= -\frac{g}{4} \frac{\Delta}{\pi \sqrt{1 + \Delta^2/4}} K \left(\frac{1 - \delta^2}{1 + \Delta^2/4} \right), \end{aligned} \quad (\text{A7})$$

where $K(m) = \Pi(0, m)$ is the complete elliptic integral of the first kind. As a function of M and θ , it becomes:

$$\begin{aligned} P_{\text{cell}}(M, \theta) &= -\frac{g}{4} \frac{M \cos \theta}{\pi \sqrt{1 + M^2 \cos^2 \theta/4}} \times \\ &\times K \left(\frac{1 - M^2 \sin^2 \theta}{1 + M^2 \cos^2 \theta/4} \right). \end{aligned} \quad (\text{A8})$$

Appendix B: SSH as a chiral insulator: no bulk and absolute winding

The SSH model is bipartite and as such possesses a chiral (sublattice) symmetry. Chiral symmetry is here of ‘‘external type’’, in contrast to the Shockley model. SSH belongs to the BDI (or to the AIII) symmetry class of the ten-fold periodic table of topological insulators and superconductors [11–13]. In 1D, as a chiral insulator, it should be characterized by a \mathbb{Z} topological invariant in the bulk, which is a winding number.

We believe that a bulk and absolute winding number can not be defined for SSH (in agreement with [48]). Let us explain why. An important ingredient of the explanation involves the different conventions (sometimes known as basis I or basis II) that can be used to define a Bloch Hamiltonian in the case of a lattice with a basis. For a general discussion of this issue, see Refs. [52–55].

Due to the chiral symmetry, the Bloch Hamiltonian for SSH only involves two out of three Pauli matrices $H(k) = h_x(k)\sigma_x + h_y(k)\sigma_y$ and its representation by an effective magnetic field $\vec{h} = (h_x, h_y, 0)$ on the Bloch sphere explores only the equator. In order to define a winding number, we need that the Bloch Hamiltonian provides a mapping from the BZ to the equator of the Bloch sphere, i.e. from S^1 to S^1 . In other words, the Bloch Hamiltonian should also be periodic with the BZ, $H(k + 2\pi) = H(k)$.

However, due to a lattice with a basis (two sites per unit cell), the canonical Bloch Hamiltonian $H_d(k)$ (basis II in the terminology of [52]), obtained from the unitary transformation $e^{-ikx} H e^{ikx}$ with x the complete position operator), see Eq. (6) with $\Delta = 0$, is *not periodic* with k . It can therefore not be used to define a winding number. For a discussion of the non-periodicity of the canonical Bloch Hamiltonian in the case of a lattice with a basis, see [55].

An alternative is to use another convention (basis I in the terminology of [52]) in order to define a periodic Bloch Hamiltonian by using the Bravais lattice position R (rather than the complete position x) operator in the unitary transformation $e^{-ikR} H e^{ikR}$. With the unit cell

choice 1 (see Fig. 2), and after projection on a subspace at fixed k , a periodic Bloch Hamiltonian reads

$$\mathcal{H}(k) = (v + w \cos k) \sigma_x - w \sin k \sigma_y, \quad (\text{B1})$$

with the expected property $\mathcal{H}(k + 2\pi) = \mathcal{H}(k)$. This periodic Bloch Hamiltonian does not contain the full information on the RM model, as it does not depend on the distance d between A and B sites. Here we have assumed that the A sites are localized exactly on the Bravais lattice positions R and the B sites are at position $R + d$ (as in Fig. 2). But the above periodic Bloch Hamiltonian does as if the B sites were also at position R , i.e. as if $d = 0$ and indeed $\mathcal{H}(k) = H_{d=0}(k)$.

There is another choice of unit cell (see choice 2 in Fig. 2) that gives another periodic Bloch Hamiltonian, which we call $\tilde{\mathcal{H}}(k)$. It reads:

$$\tilde{\mathcal{H}}(k) = (w + v \cos k) \sigma_x + v \sin k \sigma_y = H_{d=1}(k). \quad (\text{B2})$$

Upon relabeling the sites $A \leftrightarrow B$, it becomes $\tilde{\mathcal{H}}(k) \rightarrow (w + v \cos k) \sigma_x - v \sin k \sigma_y$, so that, compared to (B1), the roles of v and w are simply exchanged.

The winding number can not be computed from the non-periodic canonical Hamiltonian: $W = \emptyset$. It can be computed as $\mathcal{W} = -\Theta(w - v)$ from the periodic Bloch Hamiltonian (B1) or as $\tilde{\mathcal{W}} = \Theta(v - w) = 1 + \mathcal{W}$ from (B2), where Θ is the Heaviside step function. Such a winding number \mathcal{W} or $\tilde{\mathcal{W}}$ has no bulk physical meaning: first, it should not depend on a unit cell choice; second, it should be the same for the two dimerizations (which are identical in the bulk). The conclusion is that there is no bulk and absolute winding number for SSH, which can therefore not be characterized either as a trivial or as at topological chiral insulator.

One may argue that the band structure *topology* should only depend on the tight-binding Hamiltonian H (connectivity between orbitals, real-space topology) and not on the position operator x (spatial embedding of orbitals, real-space geometry), which may be relevant for band structure *geometry*. For example, in two dimensions, the Chern number (a topological invariant) for a band can be computed either in basis I (i.e. without the knowledge of the spatial embedding of the orbitals) or in basis II [53, 54]. Both results agree and the Chern number does not depend on a choice of unit cell. In contrast, the Berry curvature (a geometrical quantity) depends on the position of orbitals and is easily computed with standard formula only in basis II [53–55]. However, we have seen that for one-dimensional chiral insulators defined by a tight-binding model on a lattice with a basis, it is not possible to define a winding number. We have also seen that in order to compute the polarization and therefore the \mathbb{Z}_2 index $\vartheta = 2\pi P/P_q$, the connectivity of orbitals alone is not sufficient and one needs to know the spatial embedding of orbitals (the crucial information being the fact that there are two ions per unit cell and not a single ion with double charge).

The absence of a bulk winding number for SSH does not mean that it is not possible to define a winding number for a domain wall or an edge, i.e. a relative rather than absolute winding number. It therefore does not contradict the use of such a winding number to predict the existence of mid-gap states, see e.g. [48–50], which is usually called a bulk-edge correspondence. An edge-dependent winding number is defined from the periodic Bloch Hamiltonian $\mathcal{H}(k) = E_+(k)\vec{n}(k) \cdot \vec{\sigma}$ with the unit-cell choice that respects the edge. It consists in tracking whether the loop traced by the unit vector $\vec{n}(k)$ on the Bloch sphere as k spans the first Brillouin zone encloses the origin or not.

The argument predicting the presence or absence of mid-gap edge states relies on the chiral sublattice symmetry to define an edge-dependent winding number. Except at the SSH point, it does therefore not apply to the RM model. However, in-gap edge states can be present in the RM model, see Fig. 7, but they are not in the middle of the gap, at zero energy, but at $\pm\Delta$. Is there a general argument predicting the presence or absence of in-gap edge states in the RM model? It appears that each time the last bond on an edge is of weak-type (i.e.

the bond that is cut is of strong-type), an in-gap edge state is present. A more fancy way of saying the same thing is that edge states are present whenever the projection on the xy -plane of the loop traced by $\vec{n}(k)$ encloses the origin [40]. Therefore, even in the generic RM case, one invokes chiral symmetry in order to predict the existence of in-gap (and not mid-gap) edge states. A general argument for the existence of in-gap edge states for tight-binding Dirac-like Hamiltonians, without invoking chiral symmetry, is given in [56].

In summary, SSH is a trivial bulk inversion-symmetric insulator but an interface can host topologically protected mid-gap edge states. It may be seen as a 1D counterpart of 2D hexagonal boron nitride. The latter is a gapped version of graphene, with staggered on-site potential on the two sublattices of the honeycomb lattice. On the one hand, boron nitride is a trivial insulator: its Chern number vanishes as it does not break time-reversal symmetry. On the other hand, it is also a Dirac insulator as it has two gapped Dirac cones (one for each valley K/K'). A domain wall between two differently staggered domains hosts valley-filtered edge states due to the Jackiw and Rebbi mechanism, see [57].

-
- [1] N. A. Spaldin, *A beginner's guide to the modern theory of polarization*, *J. Solid State Chem.* **195**, 2 (2012).
- [2] The quantum observable associated to a classical angle can not be a hermitian operator, i.e. it is not a standard quantum observable. Berry [3] has shown that there are other types of quantum observables: geometric phases. Indeed, as shown by King-Smith, Vanderbilt and Resta [4–6], the electronic contribution to the electric polarization is given in terms of such a geometric phase, known as the Zak phase.
- [3] M. V. Berry, *Quantal Phase Factors Accompanying Adiabatic Changes*, *Proc. R. Soc. Lond. A.* **392**, 45 (1984).
- [4] R. D. King-Smith and D. Vanderbilt, *Theory of polarization of crystalline solids*, *Phys. Rev. B* **47**, 1651(R) (1993).
- [5] D. Vanderbilt and R. D. King-Smith, *Electric polarization as a bulk quantity and its relation to surface charge*, *Phys. Rev. B* **48**, 4442 (1993).
- [6] R. Resta and D. Vanderbilt, *Theory of Polarization: A Modern Approach*, in *Physics of Ferroelectrics: A Modern Perspective*, Topics in Applied Physics (Springer-Verlag, Berlin, Heidelberg, 2007), Vol. 105, pp. 21-68.
- [7] D. Xiao, M. C. Chang and Q. Niu, *Berry phase effects on electronic properties*, *Rev. Mod. Phys.* **82**, 1959 (2010).
- [8] D. Vanderbilt, *Berry phase in electronic structure theory: electric polarization, orbital magnetization and topological insulators* (Cambridge university press, 2018).
- [9] W. Shockley, *On the Surface States Associated with a Periodic Potential*, *Phys. Rev.* **56**, 317 (1939).
- [10] M. J. Rice and E. J. Mele, *Elementary Excitations of a Linearly Conjugated Diatomic Polymer*, *Phys. Rev. Lett.* **49**, 1455 (1982).
- [11] A. P. Schnyder, S. Ryu, A. Furusaki and A. W. W. Ludwig, *Classification of topological insulators and superconductors in three spatial dimensions*, *Phys. Rev. B* **78**, 195125 (2008).
- [12] A. Kitaev, *Periodic table for topological insulators and superconductors*, *AIP Conference Proceedings* **1134**, 22 (2009).
- [13] C.-K. Chiu, J. C. Y. Teo, A. P. Schnyder, and S. Ryu, *Classification of topological quantum matter with symmetries*, *Rev. Mod. Phys.* **88**, 035005 (2016).
- [14] J. Zak, *Berry's phase for energy bands in solids*, *Phys. Rev. Lett.* **62**, 2747 (1989).
- [15] T. L. Hughes, E. Prodan and B. A. Bernevig, *Inversion-symmetric topological insulators*, *Phys. Rev. B* **83**, 245132 (2011).
- [16] K. T. Chen and P. A. Lee, *Static electric field in one-dimensional insulators without boundaries*, *Phys. Rev. B* **84**, 113111 (2011).
- [17] X.-L. Qi, T. L. Hughes and S.-C. Zhang, *Topological field theory of time-reversal invariant insulators*, *Phys. Rev. B* **78**, 195424 (2008).
- [18] W. P. Su, J. R. Schrieffer, and A. J. Heeger, *Solitons in Polyacetylene*, *Phys. Rev. Lett.* **42**, 1698 (1979).
- [19] K. N. Kudin, R. Car and R. Resta, *Quantization of the dipole moment and of the end charges in push-pull polymers*, *J. Chem. Phys.* **127**, 194902 (2007).
- [20] R. Resta, *Quantum-Mechanical Position Operator in Extended Systems*, *Phys. Rev. Lett.* **80**, 1800 (1998).
- [21] F. Combes, M. Trescher, F. Piéchon and J.-N. Fuchs, *Statistical mechanics approach to the electric polarization and dielectric constant of band insulators*, *Phys. Rev. B* **94**, 155109 (2016).
- [22] C. L. Kane, Chapter 1 - *Topological Band Theory and the \mathbb{Z}_2 Invariant*, in "Topological insulators", M. Franz and L. Molenkamp editors, *Contemporary Concepts of Condensed Matter Science* **6**, 3 (2013).

- [23] A. Alexandradinata, X. Dai and B. A. Bernevig, *Wilson-Loop Characterization of Inversion-Symmetric Topological Insulators*, *Phys. Rev. B* **89**, 155114 (2014).
- [24] J. K. Asbóth, L. Oroszlány and A. Pályi, *A Short Course on Topological Insulators: Band Structure and Edge States in One and Two Dimensions*, *Lecture Notes in Physics* (919) (Springer, 2016).
- [25] B. A. Bernevig and T. Neupert, *Topological Superconductors and Category Theory*, [arXiv:1506.05805v2](https://arxiv.org/abs/1506.05805v2) (2015).
- [26] W. A. Benalcazar, B. A. Bernevig and T. L. Hughes, *Electric multipole moments, topological multipole moment pumping, and chiral hinge states in crystalline insulators*, *Phys. Rev. B* **96**, 245115 (2017).
- [27] R. Shankar, *Topological Insulators – A review*, [arxiv:1804.06471](https://arxiv.org/abs/1804.06471) (2018).
- [28] N. R. Cooper, J. Dalibard and I. B. Spielman, *Topological bands for ultracold atoms*, *Rev. Mod. Phys.* **91**, 015005 (2019).
- [29] It is crucial to impose this periodic gauge condition for the Zak phase to be gauge independent. It should also be computed using the canonical (or basis II) Bloch Hamiltonian, and not a periodic (or basis I) Hamiltonian, in order to have the desired relation with the position operator and hence with the electronic contribution to the electric polarization via the Wannier center [14, 30].
- [30] R. Resta, *Manifestations of Berry's phase in molecules and condensed matter*, *J. Phys.: Condens. Matter* **12**, R107 (2000).
- [31] In the present case, the two formulas for the polarization compare as follows: from the Zak phase, it is $P = -g \int_{-\pi}^{\pi} \frac{dk}{2\pi} [u_A^* i \partial_k u_A + u_B^* i \partial_k u_B] + g\bar{x}$, and from the charge density, $P_{\text{cell}} = -g \int_{-\pi}^{\pi} \frac{dk}{2\pi} [u_A^* x_A u_A + u_B^* x_B u_B] + g\bar{x}$, where u_l is a short notation for $u_{-,k}(x_l)$ with $l = A$ or B . The phase of the cell-periodic Bloch states plays a role in the first formula, whereas only their modulus matter in the second.
- [32] The first type of filling with only double or zero occupancy corresponds to restricted Hartree-Fock (RHF), whereas that with two edge states that have a single occupancy corresponds to unrestricted Hartree-Fock (UHF) [19].
- [33] Q. Niu, *Surface and soliton charge in insulating systems*, *Phys. Rev. B* **33**, 5368 (1986).
- [34] M. Pletyukhov, D. M. Kennes, J. Klinovaja, D. Loss and H. Schoeller, *Surface charge theorem and topological constraints for edge states: Analytical study of one-dimensional nearest-neighbor tight-binding models*, *Phys. Rev.* **101**, 165304 (2020).
- [35] The weight on the different sites is chosen such that $\sum_j \bar{q}_j = \sum_j q_j = Q_{\text{tot}} = 0$.
- [36] V. Heine, *Phase Shifts and Local Charge Neutrality in Semiconductors*, *Phys. Rev.* **145**, 593 (1966).
- [37] R. Jackiw and C. Rebbi, *Solitons with fermion number 1/2*, *Phys. Rev. D* **13**, 3398 (1976).
- [38] M. Stone, *Elementary derivation of one-dimensional fermion-number fractionalization*, *Phys. Rev. B* **31**, 6112(R) (1985).
- [39] J. Cayssol and J.-N. Fuchs, *Topological and geometrical aspects of band theory*, *J. Phys. Mater.* **4**, 034007 (2021).
- [40] S. S. Pershoguba and V. M. Yakovenko, *Shockley model description of surface states in topological insulators*, *Phys. Rev. B* **86**, 075304 (2012).
- [41] B. Bradlyn, L. Elcoro, J. Cano, M. G. Vergniory, Z. Wang, C. Felser, M. I. Aroyo and B. A. Bernevig, *Topological quantum chemistry*, *Nature* **547**, 298 (2017).
- [42] D. J. Thouless, *Quantization of particle transport*, *Phys. Rev. B* **27**, 6083 (1983).
- [43] M. Lohse, C. Schweizer, O. Zilberberg, M. Aidelsburger and I. Bloch, *A Thouless quantum pump with ultracold bosonic atoms in an optical superlattice*, *Nat. Phys.* **12**, 350 (2016).
- [44] S. Nakajima, T. Tomita, S. Taie, T. Ichinose, H. Ozawa, L. Wang, M. Troyer and Y. Takahashi, *Topological Thouless pumping of ultracold fermions*, *Nat. Phys.* **12**, 296 (2016).
- [45] M. Atala, M. Aidelsburger, J. T. Barreiro, D. Abanin, T. Kitagawa, E. Demler and I. Bloch, *Direct measurement of the Zak phase in topological Bloch bands*, *Nature Phys.* **9**, 795 (2013).
- [46] C. Dutreix, M. Bellec, P. Delplace and F. Mortessagne, *Wavefront dislocations reveal insulator topology*, *Nature Comm.* **12**, 3571 (2021).
- [47] P. St-Jean, V. Goblot, E. Galopin, A. Lemaître, T. Ozawa, L. Le Gratiet, I. Sagnes, J. Bloch and A. Amo, *Lasing in topological edge states of a one-dimensional lattice*, *Nat. Photon.* **11**, 651 (2017).
- [48] M. Guzmán, D. Bartolo and D. Carpentier, *Geometry and topology tango in chiral materials*, [arXiv:2002.02850](https://arxiv.org/abs/2002.02850) (2020).
- [49] S. Ryu and Y. Hatsugai, *Topological Origin of Zero-Energy Edge States in Particle-Hole Symmetric Systems*, *Phys. Rev. Lett.* **89**, 077002 (2002).
- [50] P. Delplace, D. Ullmo, and G. Montambaux, *Zak phase and the existence of edge states in graphene*, *Phys. Rev. B* **84**, 195452 (2011).
- [51] In [50] and in many other references, what is called a Zak phase is π times a winding number defined with respect to a specific unit cell choice imposed by an edge. Although related, it is not the geometric phase defined by Zak [14] and used in the present article.
- [52] C. Bena and G. Montambaux, *Remarks on the tight-binding model of graphene*, *New J. Phys.* **11**, 095003 (2009).
- [53] J.-N. Fuchs, F. Piéchon, M.O. Goerbig and G. Montambaux, *Topological Berry phase and semiclassical quantization of cyclotron orbits for two dimensional electrons in coupled band models*, *Eur. Phys. B* **77**, 351 (2010).
- [54] M. Fruchart, D. Carpentier and K. Gawędzki, *Parallel Transport and Band Theory in Crystals*, *Europhys. Lett.* **106**, 60002 (2014).
- [55] L.-K. Lim, J.-N. Fuchs and G. Montambaux, *Geometry of Bloch states probed by Stückelberg interferometry*, *Phys. Rev. A* **92**, 063627 (2015).
- [56] R. S. K. Mong and V. Shivamoggi, *Edge states and the bulk-boundary correspondence in Dirac Hamiltonians*, *Phys. Rev. B* **83**, 125109 (2011).
- [57] G.W. Semenoff, V. Semenoff, and Fei Zhou, *Domain Walls in Gapped Graphene*, *Phys. Rev. Lett.* **101**, 087204 (2008).